

Supplementary Information

A Dicationic Calix[4]pyrrole Derivative and its Use for the Selective Recognition and Displacement-based Sensing of Pyrophosphate

Punidha Sokkalingam,^a Dong Sub Kim,^b Hyonseok Hwang,^a Jonathan L. Sessler,^{*,b} and Chang-Hee Lee^{*,a}

Department of Chemistry and Institute of Molecular Science & Fusion Technology, Kangwon National University, Chun-Chon 200-701 Korea, ^bDepartment of Chemistry and Biochemistry, The University of Texas at Austin, Austin TX 78712 USA.

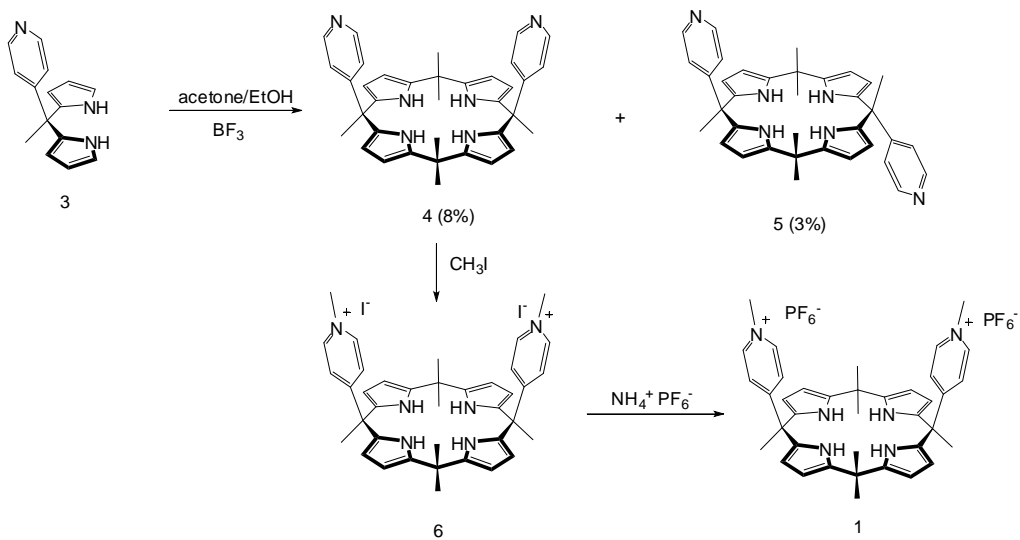
seessler@mail.utexas.edu, chhlee@kangwon.ac.kr

Table of contents	S1
Synthetic schemes	S2
Experimental section	S3
General and synthetic procedures	S4
Figure S1 ¹ H NMR spectrum of 3 in DMSO- <i>d</i> ₆ .	S6
Figure S2 ¹³ C NMR spectrum of 3 in DMSO- <i>d</i> ₆ .	S7
Figure S3 MALDI-TOF mass spectrum of 3 .	S7
Figure S4 ¹ H NMR spectrum of 4 in CDCl ₃ .	S8
Figure S5 ¹³ C NMR spectrum of 4 in CDCl ₃ .	S8
Figure S6 MALDI-TOF mass spectrum of 4 .	S9
Figure S7 ¹ H NMR spectrum of 5 in CD ₃ CN.	S9
Figure S8 ¹³ C NMR spectrum of 5 in CD ₃ CN.	S10
Figure S9 MALDI-TOF mass spectrum of 5 .	S10
Figure S10 ¹ H NMR spectrum of 1 in CD ₃ CN.	S11
Figure S11 ¹³ C NMR spectrum of 1 in CD ₃ CN.	S11
Figure S12 MALDI-TOF mass spectrum of 1 .	S12
Figure S13 Comparison of partial ¹ H NMR spectra of 4 , 5 and 1 in CD ₃ CN.	S12
Anion binding studies	S13
Figure S14 Recovery of fluorescence of [1 • 2 ⁻] upon titration with HP ₂ O ₇ ³⁻ (as the tetrabutylammonium salt) in acetonitrile at λ _{ex} = 410 nm.	S14
Figure S15 Changes in emission intensity of receptor [1 • 2 ⁻] after treatment with TBA salts of various anions in acetonitrile at λ _{ex} = 410 nm.	S14
Figure S16 Estimation of the detection limit of receptor [1 • 2 ⁻] for HP ₂ O ₇ ³⁻ .	S15
Figure S17 UV-vis absorption spectral changes of (a) 2 ⁻ upon addition of increasing concentration of 1 in acetonitrile and, (b) receptor [1 • 2 ⁻], upon addition of increasing concentrations of TBA ₃ HP ₂ O ₇ in acetonitrile.	S16
UV-vis anion binding studies: General experimental details	S17
Figure S18 (a) UV-vis absorption spectral change of 1 upon addition of TBA ₃ HP ₂ O ₇ in acetonitrile 25 °C. (b) Job plot for the interaction between host 1 and TBA ₃ HP ₂ O ₇ in acetonitrile.	S18
Figure S19 (a) UV-vis absorption spectral change of 1 upon addition of 2 ⁻ in	S19

- acetonitrile 25 °C. (b) Job plot for the interaction between host **1** and **2**⁻ in acetonitrile. S20
- Figure S20** UV-vis absorption spectral changes of **1** upon addition of (a) TBAF and (b) TBAH₂PO₄ in acetonitrile. Job plot for the interaction between host **1** and (c) TBAF and (d) TBAH₂PO₄ in acetonitrile. S21
- Figure S21** UV-vis absorption spectral changes of **1** upon addition of (a) TBACH₃COO and (b) TBACl in acetonitrile. Job plot for the interaction between host **1** and (c) TBACH₃COO and (d) TBACl in acetonitrile. S22
- Figure S22** UV-vis absorption spectral changes of **1** upon addition of (a) TBAH₂SO₄ and (b) TBABr in acetonitrile. Job plot for the interaction between host **1** and (c) TBAH₂SO₄ and (d) TBABr in acetonitrile. S23
- Figure S23** (a) UV-vis absorption spectral change of **4** upon addition of TBA₃HP₂O₇ in acetonitrile 25 °C. (b) Job plot for the interaction between host **4** and TBA₃HP₂O₇ in acetonitrile. S24
- Table S1** Affinity constants obtained from UV-vis spectroscopic titrations of receptors **4** and **1** with TBA salts of various anions in acetonitrile at 25 °C. S25
- Figure S24** MALDI-TOF mass spectra of (a) [**1**•**2**⁻] and (b) [**1**•HP₂O₇³⁻] complexes. S25
- Table S2** MALDI-TOF mass results of [**1**•**2**⁻] and [**1**•HP₂O₇³⁻] complexes. S26
- Figure S25** Partial ¹H NMR spectra of the titration of receptor **1** with HP₂O₇³⁻ (as its tetrabutylammonium salt) in CD₃CN. S26
- Figure S26** Partial ¹H NMR spectra of the titration of receptor **1** with tetrabutylammonium salt of chromenolate **2**⁻ in CD₃CN. S27
- Figure S27** Partial ¹H NMR (300 MHz) spectra of the titration of receptor [**1**•**2**⁻] with TBA salt of HP₂O₇³⁻ in CD₃CN. S28
- Figure S28** Partial ¹H NMR spectra of the titration of receptor **1** with H₂PO₄⁻ (as its tetrabutylammonium salt) in CD₃CN. S29
- Figure S29** Partial ¹H NMR spectra of receptor **1** and [**1**•HP₂O₇³⁻] upon addition of D₂O in CD₃CN. S30
- Figure S30** Spectral monitoring of the changes in the ¹H NMR spectra of CD₃CN solutions of [**1**•HP₂O₇³⁻] + 2.2 equiv. of D₂O at various time intervals. S31
- Figure S31** Plot of NH proton intensity *versus* time. Also shown here its corresponding ln *versus* time plot. S32
- Figure S32** UV-vis absorption spectral changes seen for **1** upon addition of anion in a 10-30% water-acetonitrile mixture. S33
- Figure S33** Partial ¹H NMR spectra of [**1**•HP₂O₇³⁻] upon addition of NaClO₄ in CD₃CN. S34
- Figure S34** Partial ¹H NMR spectra of [**1**•HP₂O₇³⁻] upon addition of TBAF in CD₃CN. S35
- Crystallographic Material for 1.** S36

Synthetic schemes:

1. Synthesis of 4-pyridyl picket calix[4]pyrrole **4** and receptor **1**



Experimental Section

General

¹H NMR spectra were recorded on a 400 and 300 MHz Bruker NMR spectrometer using TMS as the internal standard. Chemical shifts are reported in parts per million (ppm). When peak multiplicities are given, the following abbreviations are used: s, singlet; br s, broad singlet; d, doublet; t, triplet; m, multiplet. ¹³C NMR spectra were proton decoupled and recorded on a 100 MHz Bruker spectrometer using TMS as the internal standard. Fluorescence spectra were recorded using LS-55B (Perkin Elmer) model spectrometer. Pyrrole was distilled at atmospheric pressure from CaH₂. All other chemicals and solvents were purchased from commercial sources and were used as such, unless otherwise mentioned. Column chromatography was performed over silica gel (Merck, 230-400 mesh). All titrations (UV-vis and fluorescence) were performed using HPLC grade CH₃CN purchased from Aldrich. Compound **2** was synthesized using our previously reported procedure.⁶

Synthetic procedures

5-(4-pyridyl)-5-methyldipyrromethane 3

A solution of 4-acetylpyridine (3.0 g, 24.8 mmol) in ethanol (25 mL) was treated with pyrrole (17.2 mL, 0.24 mol) under nitrogen atmosphere. After the addition of catalytic amount of CH₃SO₃H (0.8 mL, 12.4 mmol), the mixture was refluxed for 3 days during which the color of the mixture turned dark-red. The reaction mixture was cooled to room temperature and quenched by adding aqueous NaOH (0.1 N, 50 mL) and extracted with CHCl₃ (50 mL × 2). The organic layer was dried over anhydrous Na₂SO₄ and the solvent was removed under reduced pressure to afford the crude reaction mixture, which was purified by silica gel column chromatography (CHCl₃/EtOAc = 5.5/4.5) to afford pure product **3** as brown solid. Yield: 1.47 g (25%); ¹H NMR (400 MHz, DMSO-*d*₆) δ [ppm] 10.46 (br s, 2H, pyrrole-NH), 8.47-8.45 (m, 2H, pyridyl-H), 6.99-6.97 (m, 2H, pyridyl-H), 6.70-6.68 (m, 2H, pyrrole-H), 5.94-5.92 (m, 2H, pyrrole-H), 5.60-5.58 (m, 2H, pyrrole-H), 1.99 (s, 3H, CH₃); ¹³C NMR (100 MHz, DMSO-*d*₆) δ [ppm] 157.6, 149.6, 136.6, 122.9, 117.9, 106.8, 106.6, 44.5, 27.4; MALDI-MS Calcd. for C₁₅H₁₅N₃ 237.13, Found 238.17 (M+1).

5,15-(4-pyridyl)-5,10,10,15,20,20-hexamethylcalix[4]pyrrole 4:

To the solution of compound **3** (1.0 g, 4.21 mmol) in acetone/ethanol mixture (1:1, 30 mL) was added $\text{BF}_3 \cdot \text{OEt}_2$ (1.0 mL, 8.43 mmol) and the mixture was stirred for 24 h at room temperature. The reaction mixture was quenched upon addition of triethylamine (2.53 mL, 18.12 mmol). Excess acetone was removed under reduced pressure and the mixture was combined with water and extracted with CH_2Cl_2 (100 mL \times 2). The organic layer was dried over anhydrous Na_2SO_4 and the solvent was removed in *vacuo*. Column chromatography over silica gel afforded a clear separation of two isomers. The first minor fraction containing *trans* isomer (0.07 g, 3%) was collected using a $\text{CHCl}_3/\text{CH}_3\text{OH}$ (9.9/0.1). While the second major fraction containing the required *cis* isomer **4** was collected as a white solid using a $\text{CHCl}_3/\text{CH}_3\text{OH}$ (9.8/0.2) as a eluent. Yield: 0.19 g (8%); ^1H NMR (400 MHz, CDCl_3) δ [ppm] 8.46-8.45 (m, 4H, pyridyl-H), 7.26 (br s, 4H, pyrrole-NH), 6.91-6.89 (m, 4H, pyridyl-H), 5.95-5.94 (m, 4H, pyrrole-H), 5.63-5.61 (m, 4H, pyrrole-H), 1.88 (s, 6H, CH_3), 1.63 (s, 6H, CH_3), 1.55 (s, 6H, CH_3); ^{13}C NMR (100 MHz, CDCl_3) δ [ppm] 156.7, 149.4, 138.8, 134.9, 122.5, 106.3, 103.5, 44.5, 35.2, 30.0, 27.8, 27.1; MALDI-MS Calcd. for $\text{C}_{36}\text{H}_{38}\text{F}_2\text{N}_6$ 554.32, Found 555.29 (M+1).

Compound 1

To a solution of **4** (0.15 g, 0.27 mmol) in anhydrous dichloromethane (10 mL), CH_3I (1.68 mL, 2.70 mmol) was added. The reaction mixture was stirred at room temperature for 24 h. The yellow colored precipitated solids were isolated by filtration and washed with CH_2Cl_2 (10 mL \times 3) to give a pure diiodide salt **5** (0.14 g, 60%). ^1H NMR (400 MHz, CD_3CN) δ [ppm] 9.61 (br s, 4H, pyrrole-NH), 8.40 (d, $J = 6.8$ Hz, 4H, pyridyl-H), 7.46 (d, $J = 6.7$ Hz, 4H, pyridyl-H), 5.99-5.98 (m, 4H, pyrrole-H), 5.81-5.80 (m, 4H, pyrrole-H), 4.15 (s, 3H, $\text{N}^+\text{-CH}_3$), 4.12 (s, 3H, $\text{N}^+\text{-CH}_3$), 1.89 (s, 6H, CH_3), 1.73 (s, 6H, CH_3), 1.70 (s, 6H, CH_3); ^{13}C NMR (100 MHz, CD_3CN) δ [ppm] 170.1, 145.0, 141.6, 134.3, 127.6, 105.8, 102.4, 47.7, 46.0, 35.1, 31.2, 29.0, 26.8; MALDI-MS Calcd. for $\text{C}_{38}\text{H}_{44}\text{I}_2\text{N}_6$ 838.17, Found 711.26 (M-I). The pure diiodide salt **5** (0.12 g, 0.14 mmol) was dissolved in 2 mL hot acetonitrile. Then an aqueous solution of NH_4PF_6 was added in one portion for the anion exchange reaction. The reaction mixture was stirred for 1 h at room temperature. This gave rise to a light yellow precipitate, which was filtered off and washed with 100 mL water. The crude product was then recrystallized from acetonitrile and water and afforded the pure receptor **1** in the form of light yellow crystals in 52% yield (65 mg).

^1H NMR (400 MHz, CD_3CN) δ [ppm] 8.44 (d, $J = 6.7$ Hz, 4H, pyridyl-H), 7.96 (br s, 4H, pyrrole-NH), 7.48 (d, $J = 6.7$ Hz, 4H, pyridyl-H), 5.96-5.95 (m, 4H, pyrrole-H), 5.68-5.66 (m, 4H, pyrrole-H), 4.22 (s, 6H, $\text{N}^+\text{-CH}_3$), 1.95 (s, 6H, CH_3), 1.66 (s, 6H, CH_3), 1.53 (s, 6H, CH_3); ^{13}C NMR (100 MHz, CD_3CN) δ [ppm] 167.3, 144.3, 139.9, 132.7, 126.0, 106.2, 103.2, 47.2, 45.3, 34.7, 29.1, 26.3, 25.9; MALDI-MS Calcd. for $\text{C}_{38}\text{H}_{44}\text{I}_2\text{N}_6$ 874.29, Found 729.31 (M- PF_6).

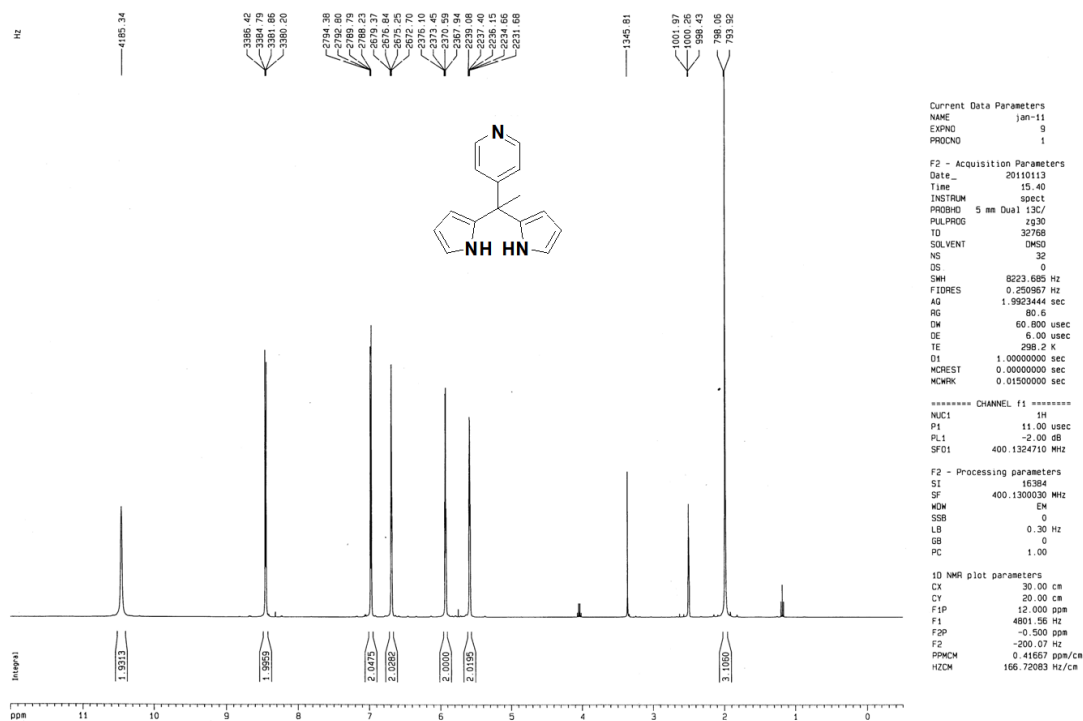


Figure S1. ¹H NMR (400 MHz) spectrum of 3 in DMSO-*d*₆.

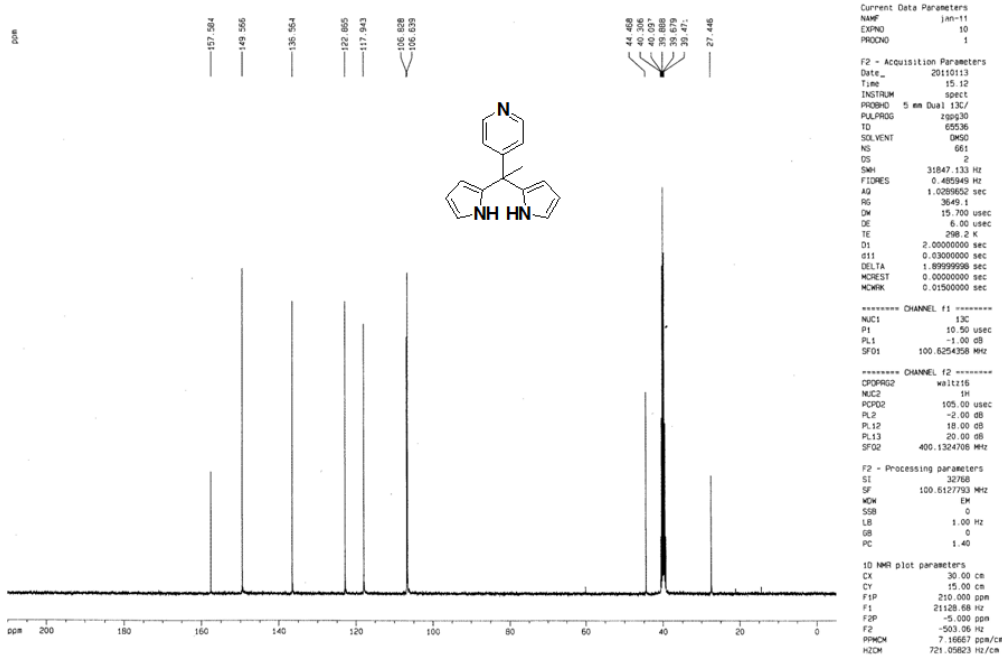


Figure S2. ¹³C NMR (100 MHz) spectrum of 3 in DMSO-*d*₆.

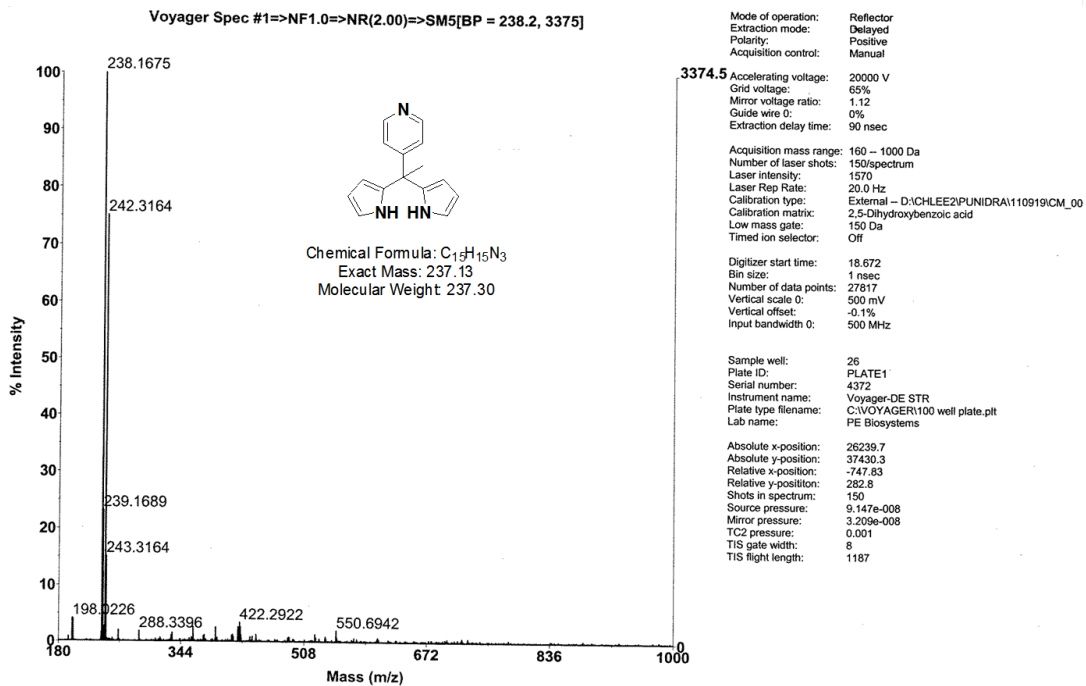


Figure S3. MALDI-TOF mass spectrum of **3**.

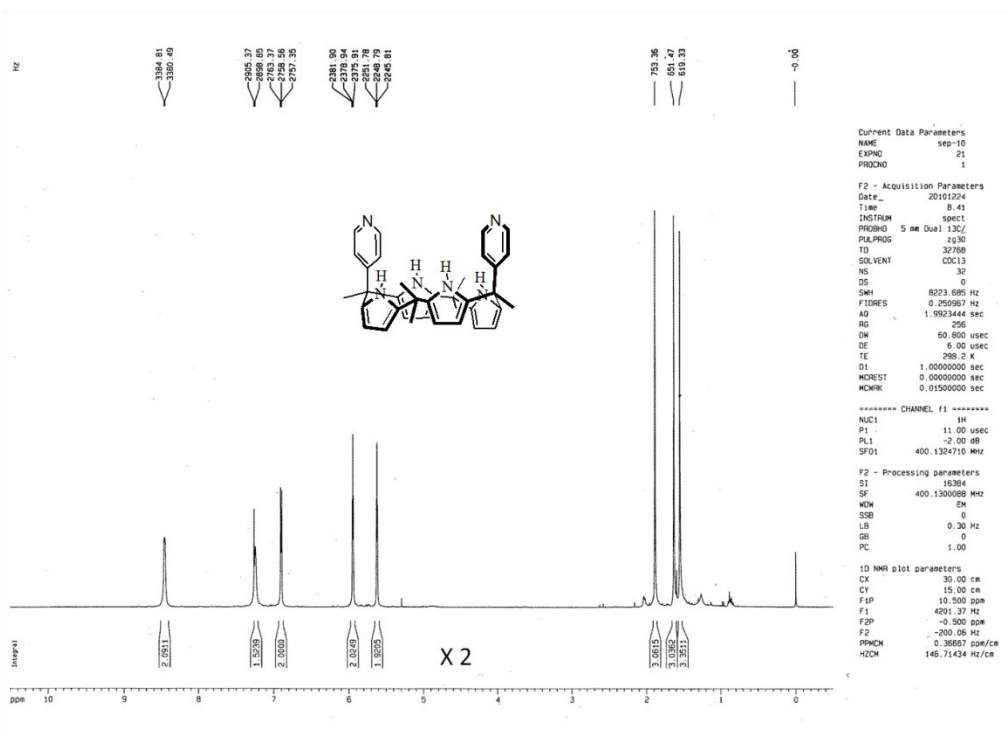


Figure S4. ¹H NMR (400 MHz) spectrum of **4** in CDCl₃.

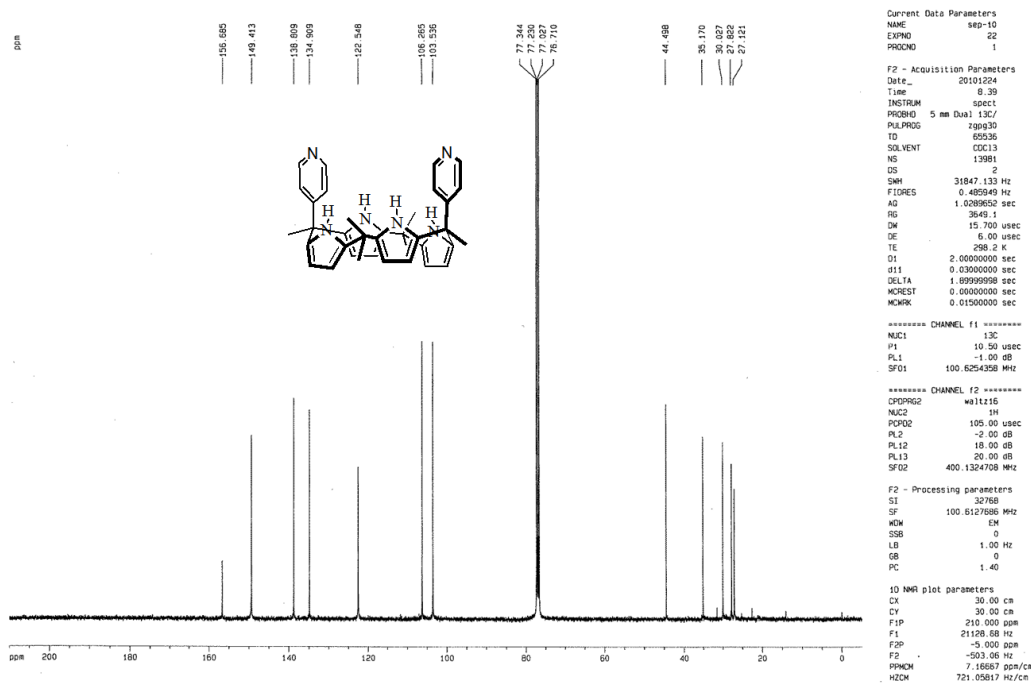


Figure S5. ^{13}C NMR (100 MHz) spectrum of **4** in CDCl_3 .

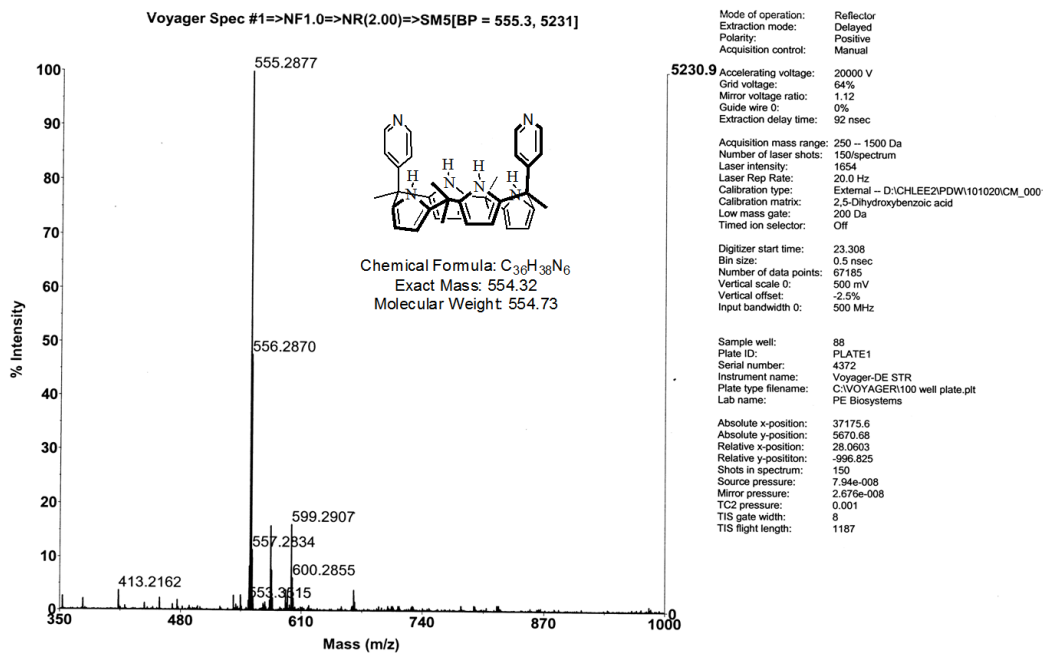


Figure S6. MALDI-TOF mass spectrum of **4**.

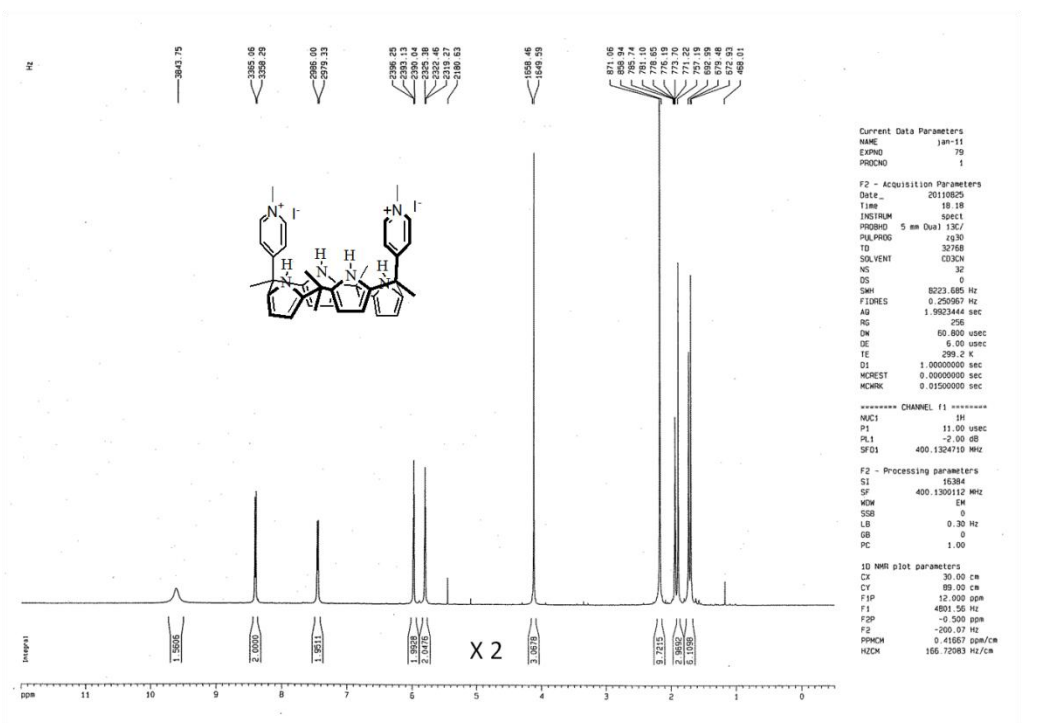


Figure S7. ¹H NMR (400 MHz) spectrum of **5** in CD₃CN.

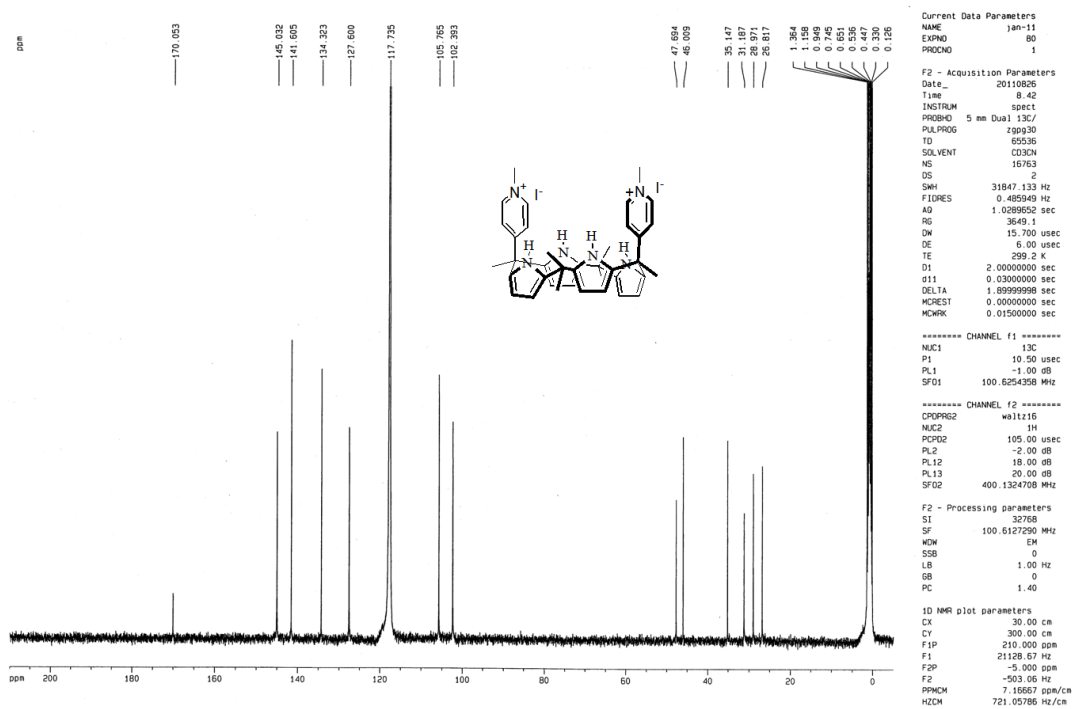


Figure S8. ¹³C NMR (100 MHz) spectrum of **5** in CD₃CN.

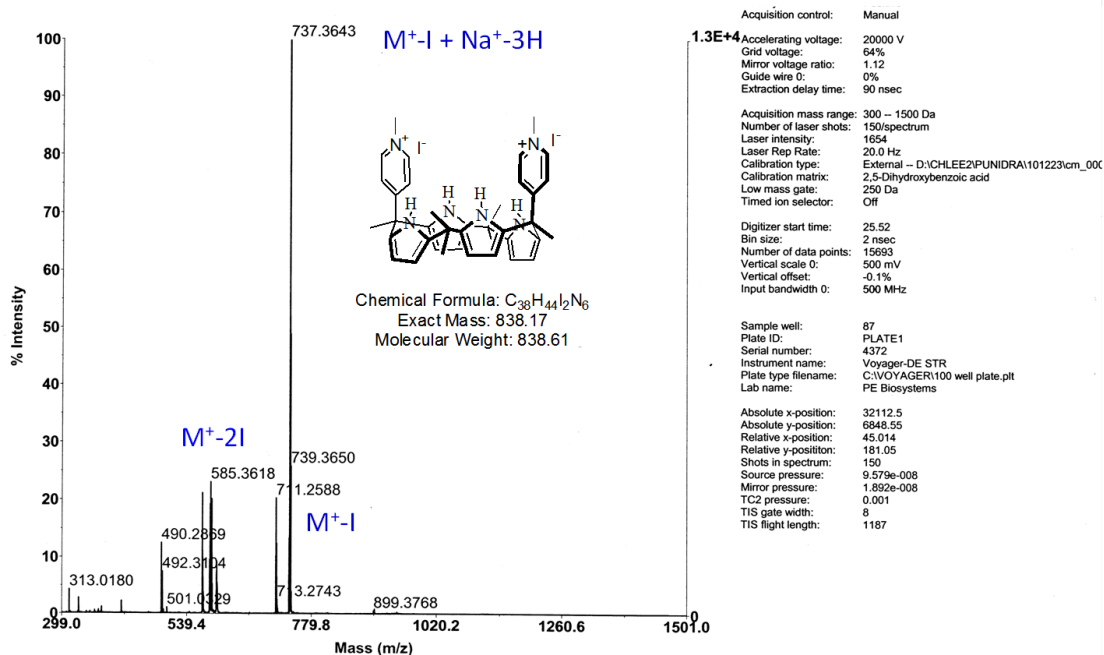


Figure S9. MALDI-TOF mass spectrum of 5.

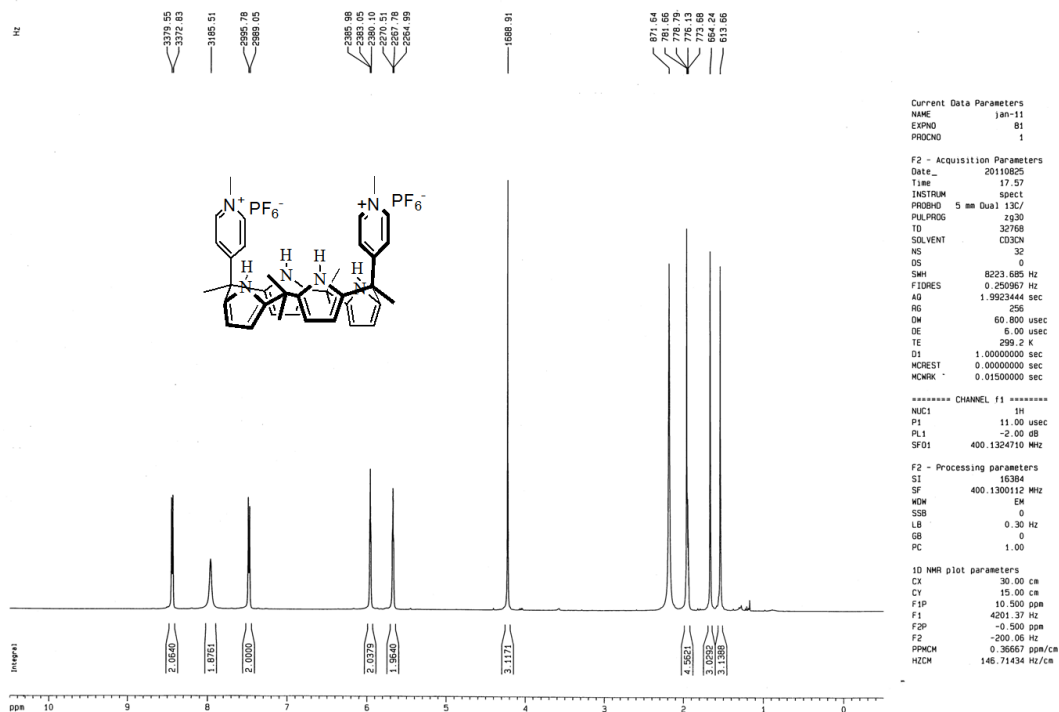


Figure S10. ¹H NMR (400 MHz) spectrum of 1 in CD₃CN.

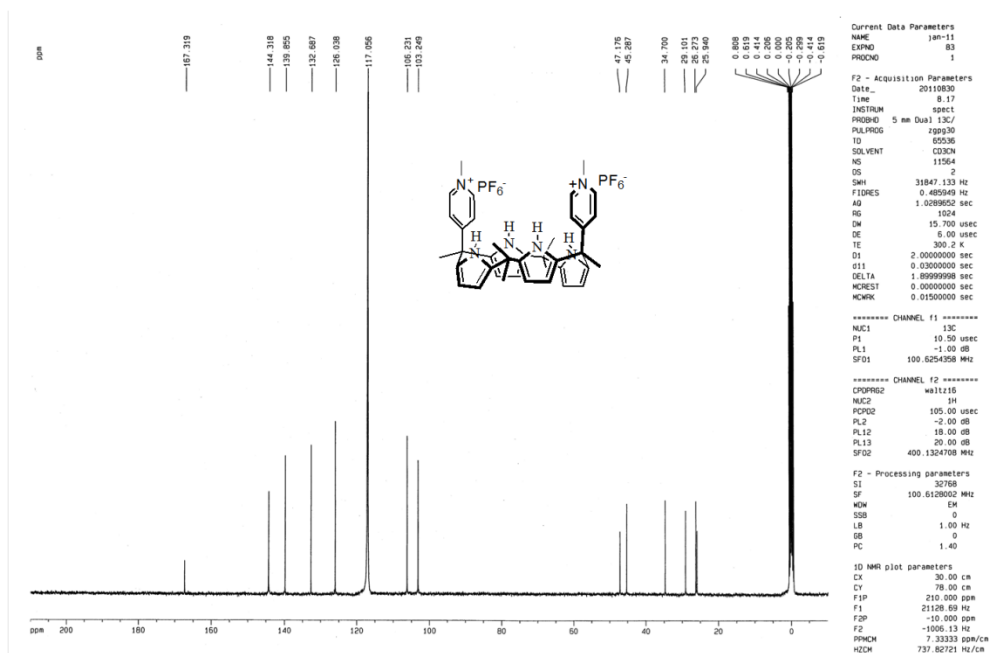


Figure S11. ^{13}C NMR (100 MHz) spectrum of **1** in CD_3CN .

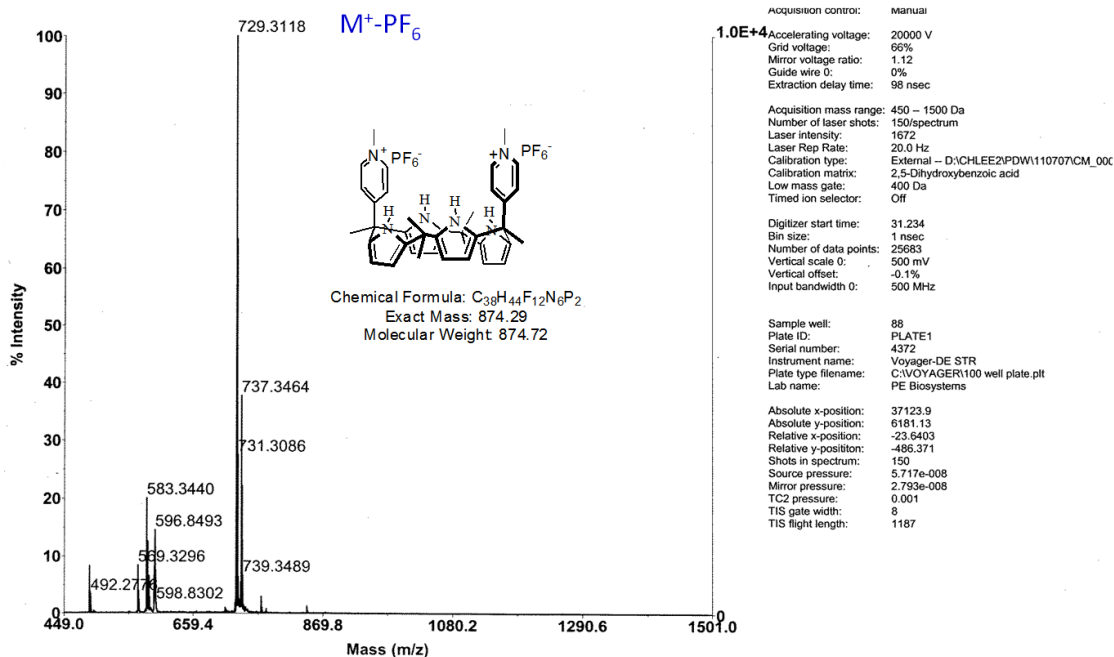


Figure S12. MALDI-TOF mass spectrum of **1**.

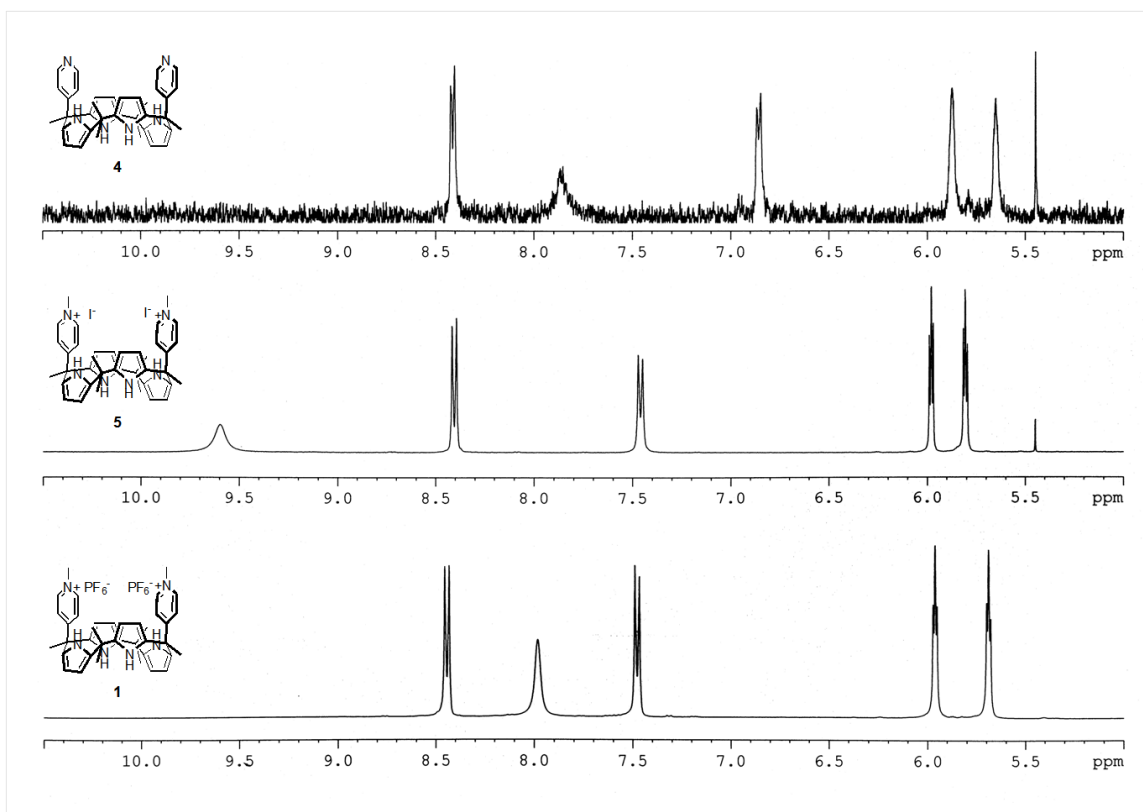


Figure S13. Comparison of partial ^1H NMR (300 MHz) spectra of (top) **4**, (middle) **5** and (bottom) **1** in CD_3CN . The comparison clearly indicates that the counter anion (PF_6^-) of receptor **1** is not involved in hydrogen bonding with the pyrrole-NHs and therefore the anion will not interfere the other anions used in the various binding studies.

Anion binding studies

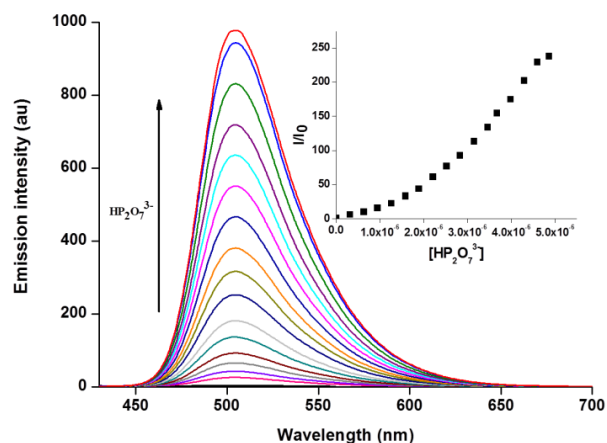


Figure S14. Recovery of fluorescence of [1•2] upon titration with $\text{HP}_2\text{O}_7^{3-}$ (as its tetrabutyl ammonium salt, 0 - 4.9 μM) in acetonitrile at $\lambda_{\text{ex}} = 410$ nm, [1] = 4.8 μM , [2] = 2.1 μM ; Inset shows a plot of I/I_0 versus $\text{TBA}_3\text{HP}_2\text{O}_7$ concentration.

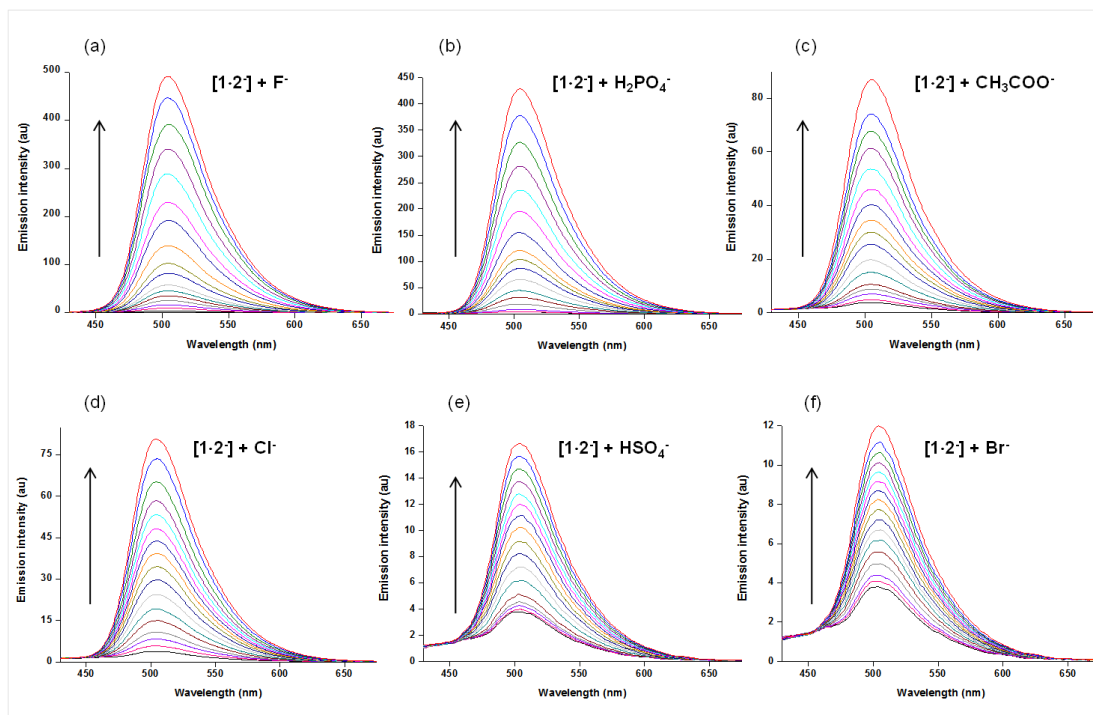


Figure S15. Changes in emission intensity of receptor [1•2] (solution of tetrabutylammonium salt of chromenolate 2⁻ (2.1 μM) and 1 (4.8 μM)) upon titration with TBA salts of various anions (0 - 4.9 μM) in acetonitrile at $\lambda_{\text{ex}} = 410$ nm.

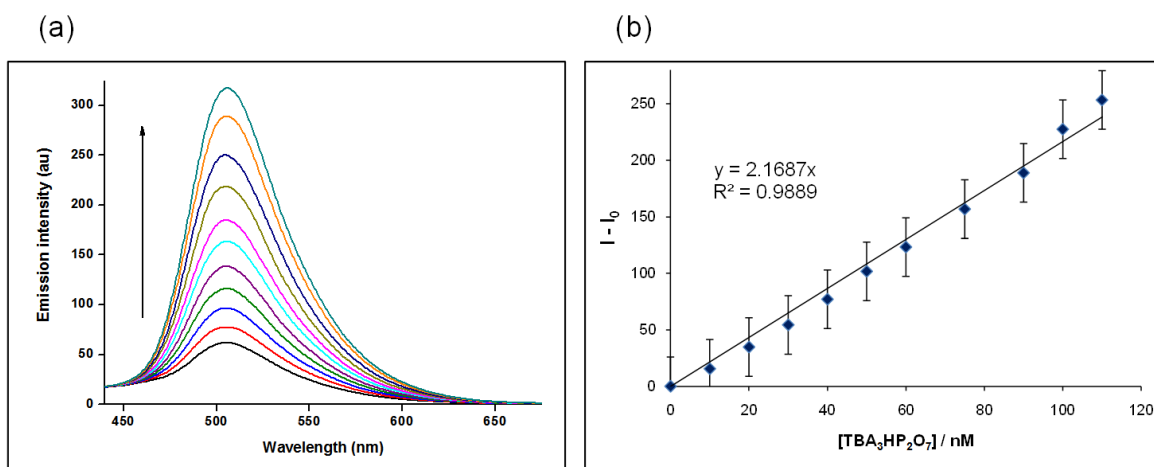


Figure S16. Estimation of the detection limit of receptor [1•2⁻] for HP₂O₇³⁻. (a) Fluorescence spectral change ($\lambda_{\text{ex}} = 410$ nm) of [1•2⁻] (solution of **1** (4.8 μM) and **2⁻** (2.1 μM)) upon addition of TBA₃HP₂O₇ (0-110 nM) in acetonitrile. (b) Plot of the emission intensity ($\lambda_{\text{em}} = 500$ nm) versus TBA₃HP₂O₇ concentration. Error bars represent standard deviations of three experiments. Note that, only for this experiment, an emission slit width of 15 nm was used to permit more sensitive detection (an emission slit width of 5 nm was used for data shown in other figures).

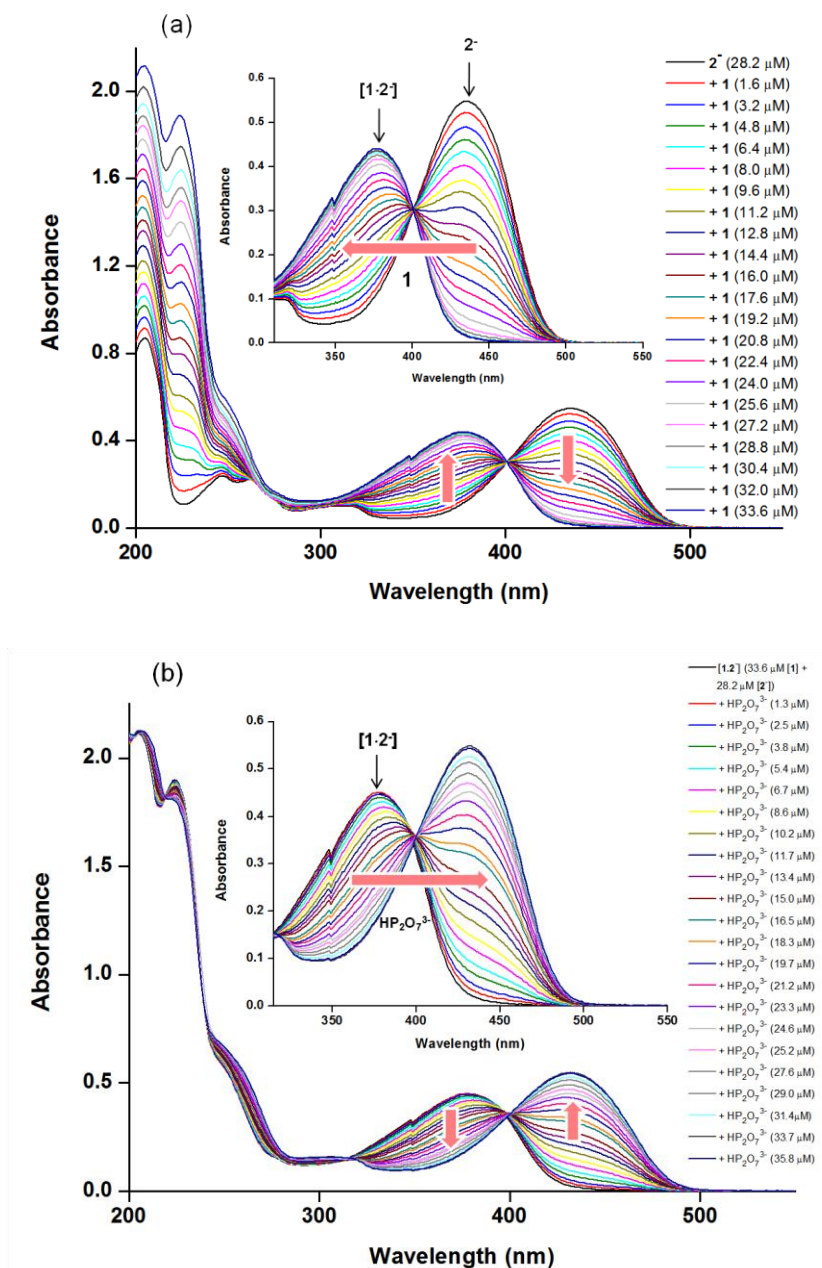


Figure S17. UV-vis absorption spectral changes of (a) 2^- (28.2 μM) upon addition of increasing concentration of 1 (0 – 33.6 μM) in acetonitrile (blue shifts from 434 nm to 378 nm) and (b) receptor $[1\cdot 2^-]$, upon addition of increasing concentrations of $\text{TBA}_3\text{HP}_2\text{O}_7$ (0 – 35.8 μM) in acetonitrile [red shifts from 378 nm to 434 nm]. Reappearance of original chromenolate 2^- spectrum due to displacement of the prebound anion 2^- from 1 via the added pyrophosphate anion.

UV-vis anion binding studies

Experimental details

Stock solutions of the receptor **1** being studied were made up in acetonitrile with the final concentrations being 1×10^{-5} M. The anion solutions used to effect the titration contained the same concentration as the receptor solutions into which they were being titrated in order to eliminate dilution effects that arise during the titrations.

The general procedure for the UV-vis binding studies involved making sequential additions of anionic guests to a 2.5 mL aliquot of the host stock solution in a spectrometric cell. The data was then collated and combined to produce plots that showed the changes in host spectral features as a function of guest concentration.

Job plot construction

Stock solutions of the receptor **1** (1.0×10^{-5} M) and TBA₃HP₂O₇ (1.0×10^{-5} M) were prepared separately in acetonitrile. For the F⁻ and H₂PO₄⁻, stock solutions of the host **1** (2.0×10^{-5} M) and the tetrabutylammonium anion salts (2.0×10^{-5} M) were prepared separately in acetonitrile. For the remaining anions, stock solutions of the host **1** (3.0×10^{-5} M) and the tetrabutylammonium anion salts (3.0×10^{-5} M) were prepared separately in acetonitrile. For control experiment, stock solutions of the host **4** (3.0×10^{-5} M) and TBA₃HP₂O₇ (3.0×10^{-5} M) were prepared separately in acetonitrile. The UV-vis spectrum was taken for each of 11 different solutions containing a total of 2.5 mL of the receptor **1** and tetrabutylammonium salt in the following ratios: 2.5:0, 2.25:0.25, 2.0:0.5, 1.75:0.75, 1.5:1.0, 1.25:1.25, 1.0:1.5, 0.75:1.75, 0.5:2.0, 0.25:2.25 and 0:2.5. Job plots were constructed by plotting ΔA observed at 243 nm against $[\text{host}] / ([\text{host}] + [\text{guest}])$.

Calculations of affinity constants, K_a

Upon addition of tetrabutylammonium salts, the UV spectra changed gradually. These changes were ascribed to anion binding, with the corresponding association constants (K_a) being determined by nonlinear curve fitting of the curves obtained by plotting the absorbance changes ΔA observed at 243 nm against the concentration of the tetrabutylammonium anion salt added, [X]. The data was fitted to the equation,

$$\Delta A = A \cdot \{([1] + [X^-] + (1/K_a)) - \{([1] + [X^-] + (1/K_a))^2 - (4 \cdot [1] \cdot [X^-])\}^{1/2}\} / (2 \cdot [1])$$

where, the one unknown parameter is K_a , the value of the association constant; this value was obtained by the fit to the data with good fits (e.g., $R^2 \geq 0.99$) being obtained unless noted otherwise.

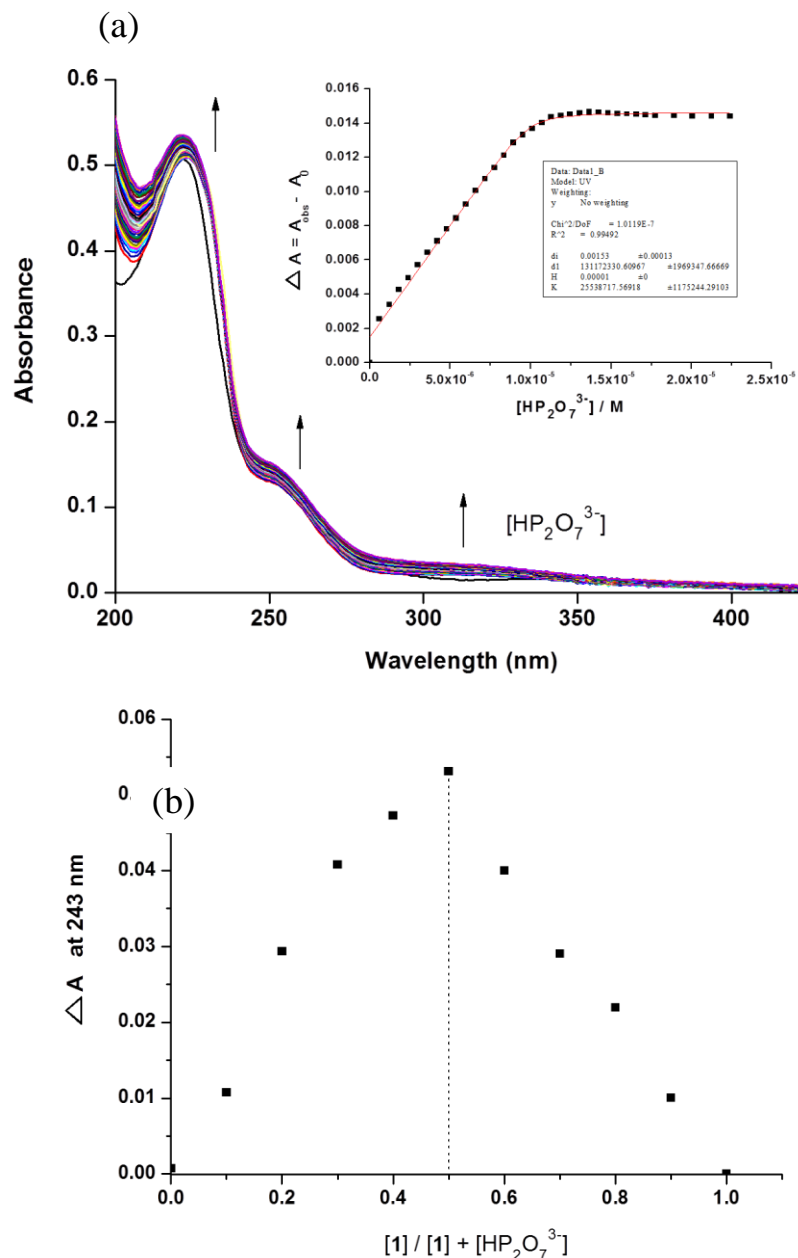


Figure S18. (a) UV-vis absorption spectral change of **1** (1.00×10^{-5} M) upon addition of TBA₃HP₂O₇ (0 to 3 equiv.) in acetonitrile 25 °C. Inset shows the corresponding titration curve (plot of change in absorbance at 243 nm *versus* TBA₃HP₂O₇). (b) Job plot for the interaction between host **1** and TBA₃HP₂O₇ in acetonitrile with [host + guest] = 1.00×10^{-5} M. A maximum value at 0.5 is seen; this is consistent with a 1:1 (host: guest) binding stoichiometry.

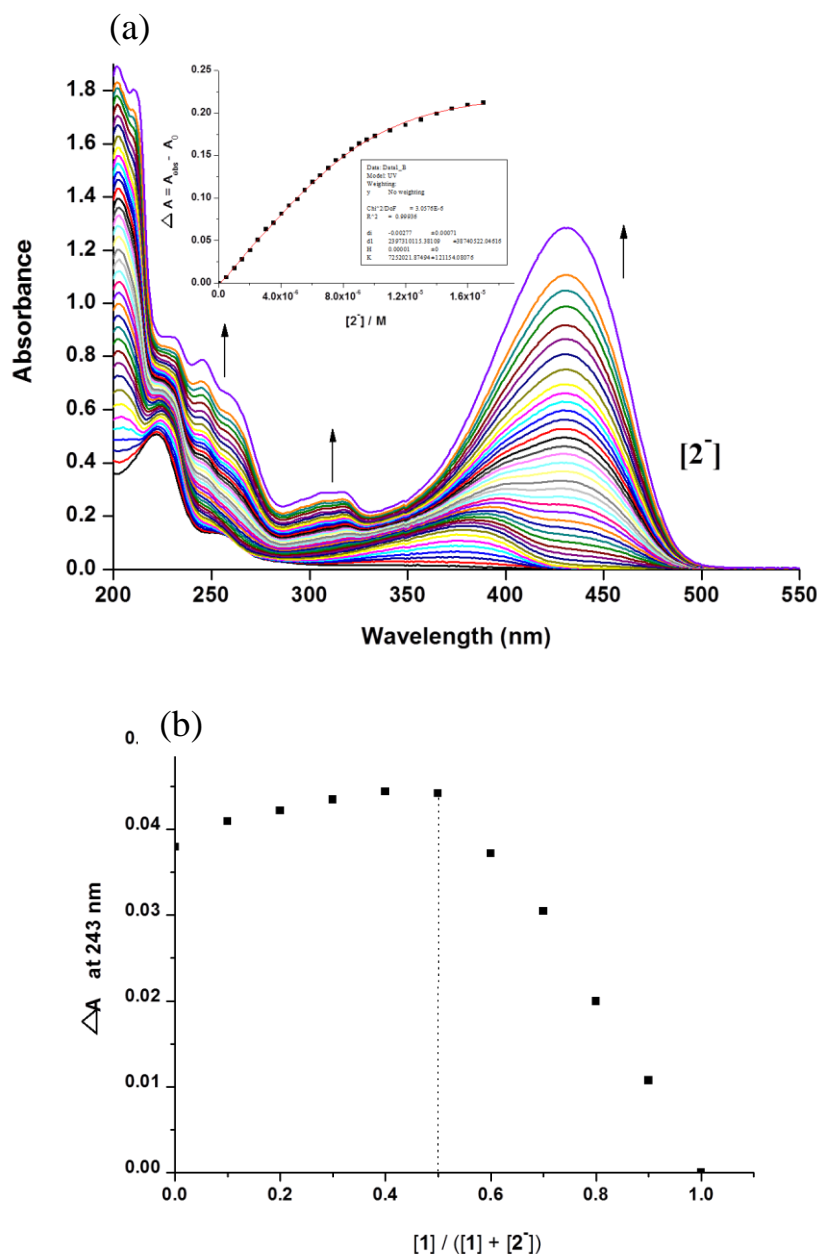


Figure S19. (a) UV-vis absorption spectral change of **1** (1.00×10^{-5} M) upon addition of **2⁻** (0 to 3 equiv.) in acetonitrile 25 °C. Inset shows the corresponding titration curve (plot of change in absorbance at 243 nm *versus* **2⁻**). Note that, absorption changes occurred only up to 1.7 equiv of **2⁻** added, were used to plot titration curve since free coumarin unit also exhibits the absorption at 243 nm. (b) Job plot for the interaction between host **1** and **2⁻** in acetonitrile with $[host + guest] = 1.00 \times 10^{-5}$ M. A maximum value at 0.5 is seen; this is consistent with a 1:1 (host: guest) binding stoichiometry.

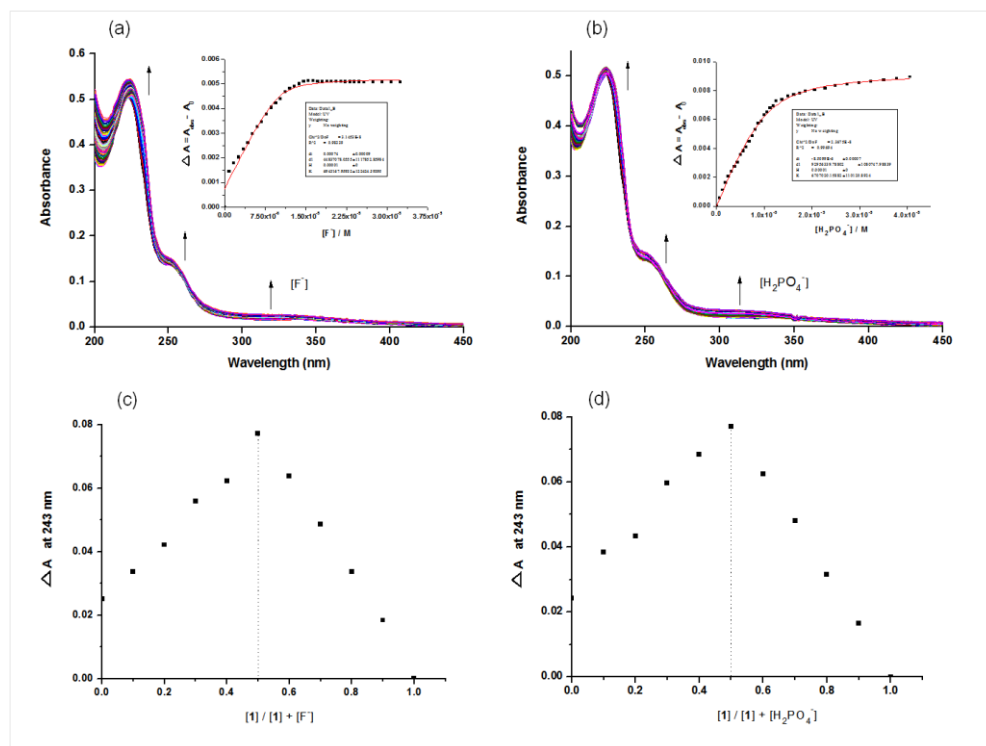


Figure S20. UV-vis absorption spectral changes of **1** (1.00×10^{-5} M) upon addition of 0 to 4 equiv. of (a) TBAF and (b) TBAH₂PO₄ in acetonitrile 25 °C. Inset shows their corresponding titration curves (plot of change in absorbance at 243 nm *versus* tetrabutylammonium salt of anions). Job plot for the interaction between host **1** and (c) TBAF and (d) TBAH₂PO₄ in acetonitrile with [host + guest] = 2.00×10^{-5} M. A maximum values at 0.5 are seen in both the cases; this is consistent with a 1:1 (host: guest) binding stoichiometries.

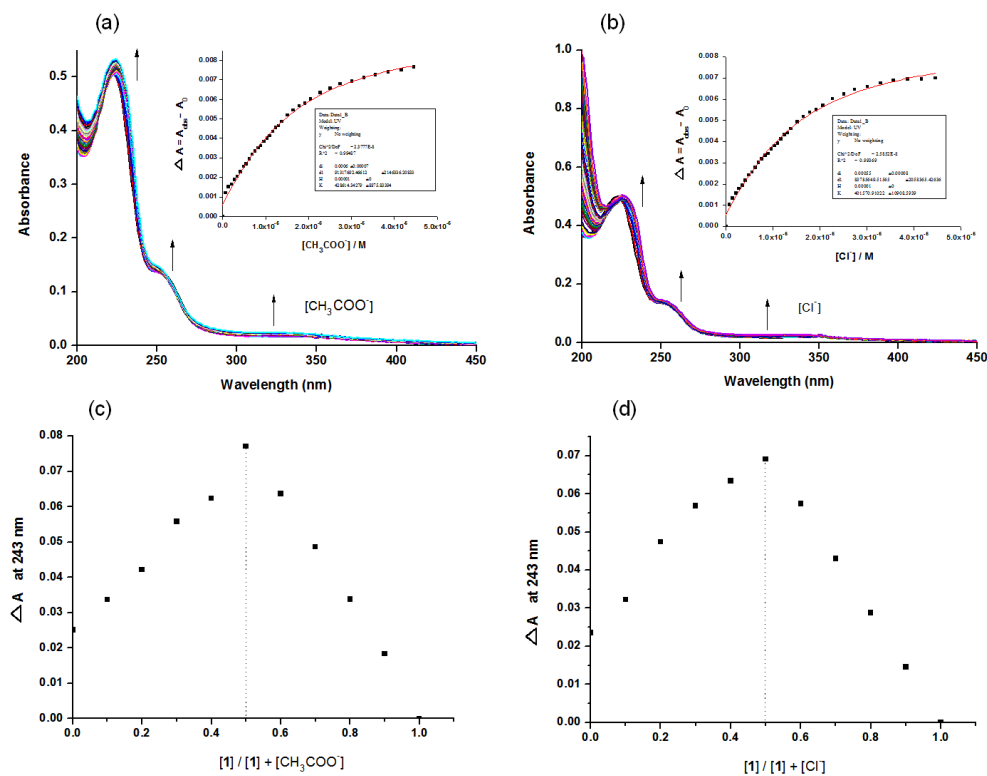


Figure S21. UV-vis absorption spectral changes of **1** (1.00×10^{-5} M) upon addition of 0 to 4.5 equiv. of (a) TBACH₃COO and (b) TBACl in acetonitrile 25 °C. Inset shows their corresponding titration curves (plot of change in absorbance at 243 nm *versus* tetrabutylammonium salt of anions). Job plot for the interaction between host **1** and (c) TBACH₃COO and (d) TBACl in acetonitrile with [host + guest] = 3.00×10^{-5} M. Maximum values at 0.5 are seen in both the cases; this is consistent with a 1:1 (host: guest) binding stoichiometries.

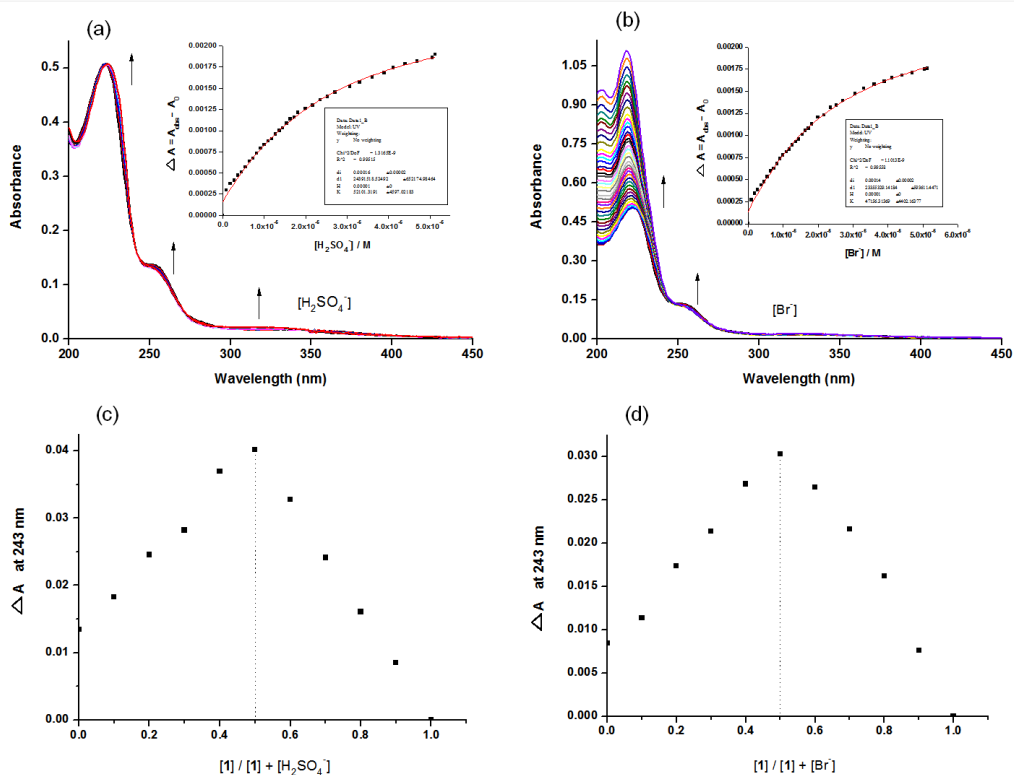


Figure S22. UV-vis absorption spectral changes of **1** (1.00×10^{-5} M) upon addition of 0 to 5 equiv. of (a) TBAH₂SO₄ and (b) TBABr in acetonitrile 25 °C. Inset shows their corresponding titration curves (plot of change in absorbance at 243 nm *versus* tetrabutylammonium salt of anions). Job plot for the interaction between host **1** and (c) TBAH₂SO₄ and (d) TBABr in acetonitrile with [host + guest] = 3.00×10^{-5} M. Maximum values at 0.5 are seen in both the cases; this is consistent with a 1:1 (host: guest) binding stoichiometries.

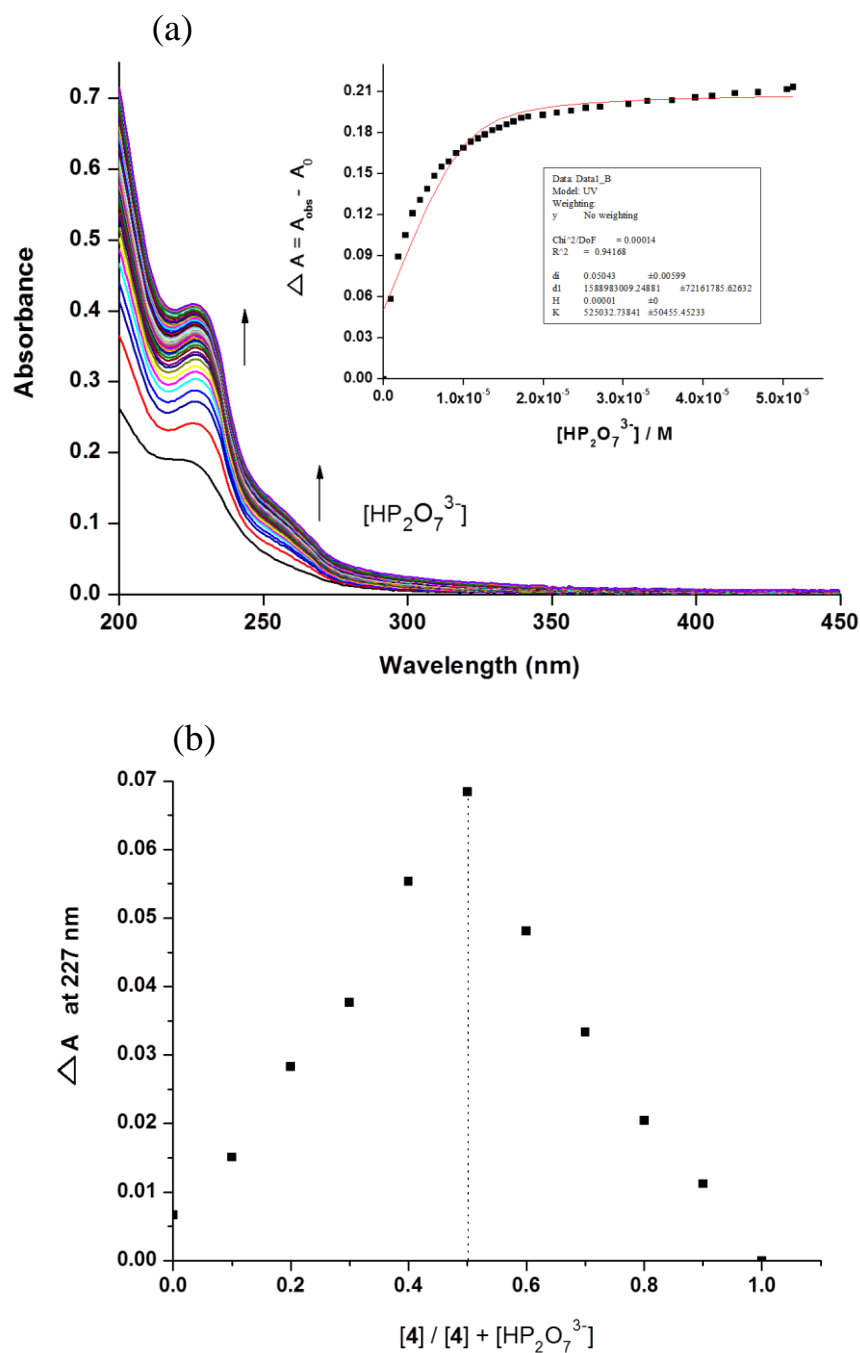


Figure S23. (a) UV-vis absorption spectral change of **4** (1.00 × 10⁻⁵ M) upon addition of TBA₃HP₂O₇ (0 to 5 equiv.) in acetonitrile 25 °C. Inset shows the corresponding titration curve (plot of change in absorbance at 227 nm versus TBA₃HP₂O₇). (b) Job plot for the interaction between host **4** and TBA₃HP₂O₇ in acetonitrile with [host + guest] = 3.00 × 10⁻⁵ M. Maximum value at 0.5 is seen; this is consistent with a 1:1 (host: guest) binding stoichiometry.

Table S1. Affinity constants obtained from UV-vis spectroscopic titrations of receptors **4** and **1** with TBA salt various anions in acetonitrile at 25 °C. $[1] = [4] = 1.00 \times 10^{-5}$ M.

Receptor	Anion	Binding constant K_a/M^{-1}
4	$HP_2O_7^{3-}$	$(5.25 \pm 0.50) \times 10^5$
1	$HP_2O_7^{3-}$	$(2.55 \pm 0.12) \times 10^7$
1	2⁻	$(7.25 \pm 0.12) \times 10^6$
1	F ⁻	$(6.94 \pm 0.12) \times 10^6$
1	$H_2PO_4^-$	$(6.71 \pm 0.11) \times 10^6$
1	CH_3COO^-	$(4.29 \pm 0.09) \times 10^5$
1	Cl ⁻	$(4.02 \pm 0.11) \times 10^5$
1	HSO_4^-	$(5.21 \pm 0.46) \times 10^4$
1	Br ⁻	$(4.72 \pm 0.44) \times 10^4$

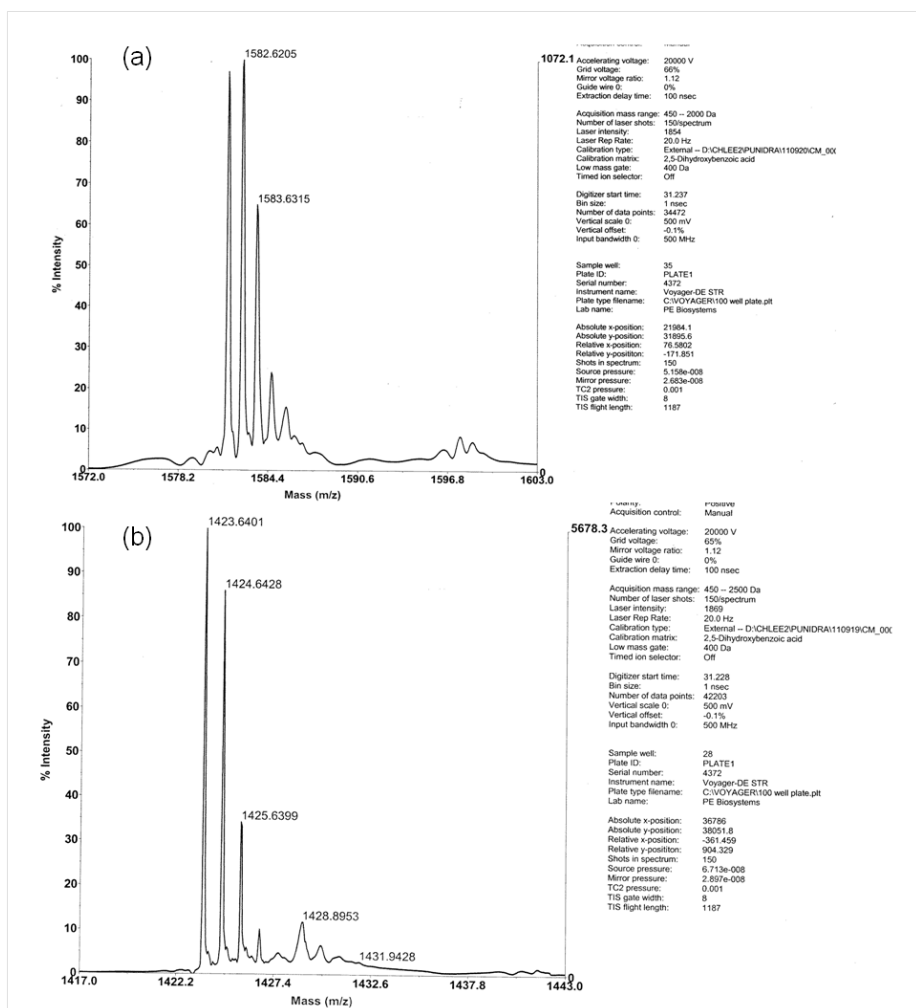


Figure S24. MALDI-TOF mass spectra (a) $[1\cdot 2^-]$ and (b) $[1\cdot \text{HP}_2\text{O}_7^{3-}]$ complexes.

Table S2. MALDI-TOF mass results of $[1\cdot 2^-]$ and $[1\cdot \text{HP}_2\text{O}_7^{3-}]$ complexes.

	Host : Guest	Complex	Calculated (<i>m/z</i>)	Found (<i>m/z</i>)
(a)	1:1	$[1\cdot 2^-] + \text{TBA}^+$ $\text{C}_{80}\text{H}_{120}\text{F}_{15}\text{N}_8\text{O}_3\text{P}_2$	1587.87	1582.62
(b)	1:1	$[1\cdot \text{HP}_2\text{O}_7^{3-}] - \text{PF}_6 + 2\text{TBA}^+ + \text{K}^+$ $\text{C}_{70}\text{H}_{117}\text{F}_6\text{N}_8\text{O}_7\text{P}_3\text{K}$	1427.78	1423.64

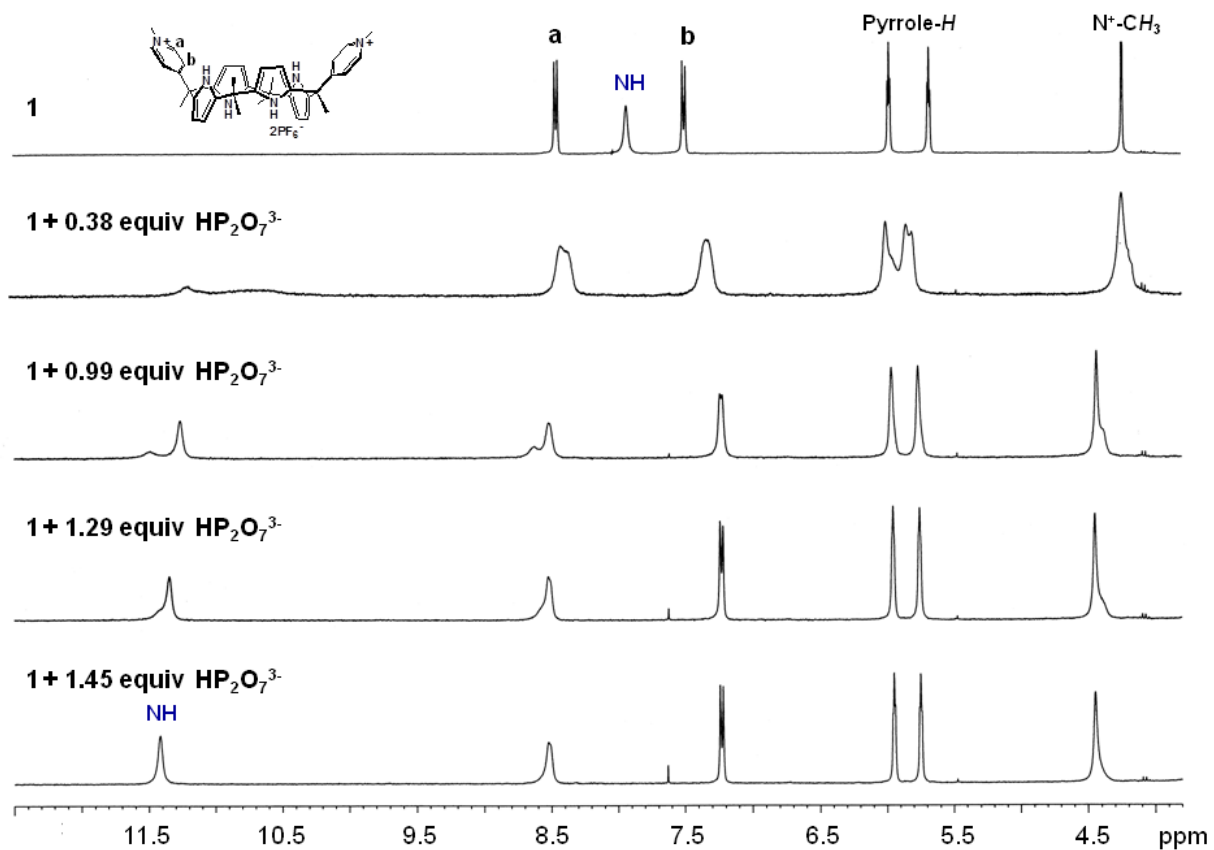


Figure S25. Partial ^1H NMR (300 MHz) spectra of the titration of receptor **1** (4.57 mM) with $\text{HP}_2\text{O}_7^{3-}$ (as its tetrabutylammonium salt) in CD_3CN .

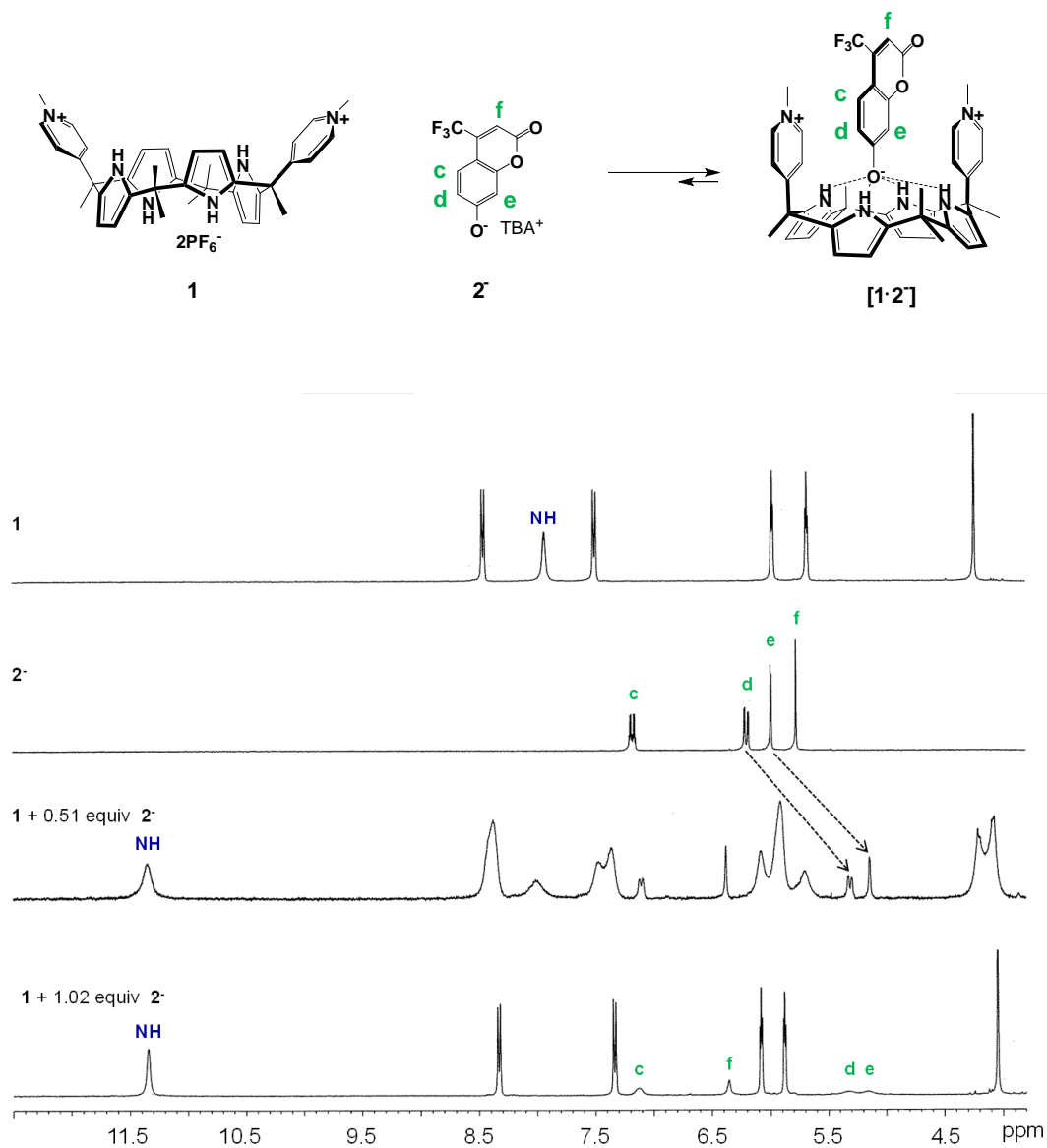


Figure S26. Partial ¹H NMR (300 MHz) spectra of the titration of receptor **1** (4.57 mM) with tetrabutylammonium salt of chromenolate **2**⁻ in CD₃CN. Partial ¹H NMR spectrum of **2**⁻ (4.66 mM) is also shown for comparison.

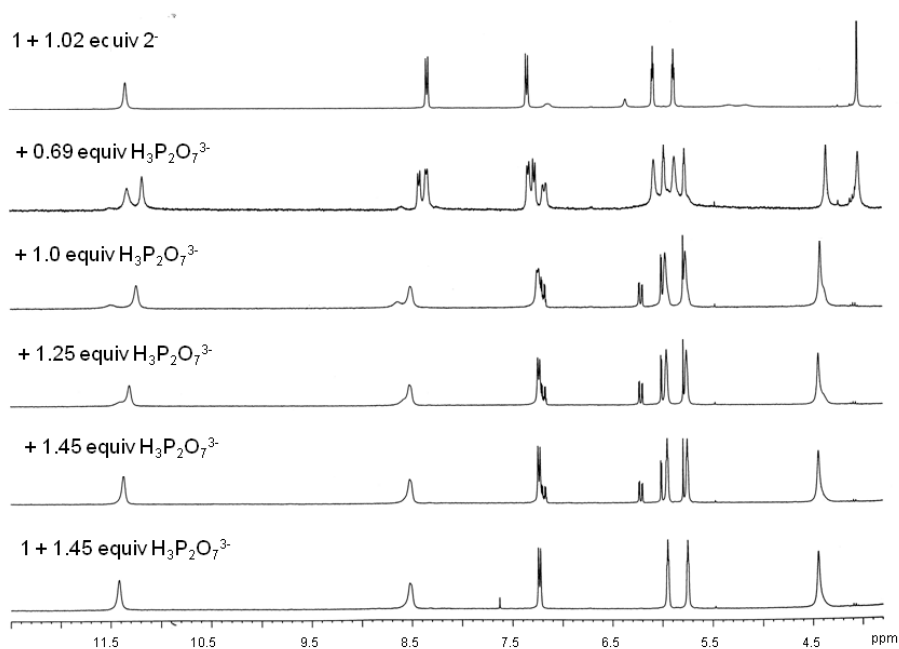


Figure S27. Partial ¹H NMR (300 MHz) spectra of the titration of receptor [1•2⁻] (1 (4.57 mM) + 1.02 equiv. of 2⁻) with the TBA salt of HP₂O₇³⁻ in CD₃CN. The spectrum marked with arrow indicates the complete displacement of 2⁻ from 1 by the added HP₂O₇³⁻. Partial ¹H NMR spectrum of [1•HP₂O₇³⁻] (1 (4.57 mM) + 1.45 equiv. of HP₂O₇³⁻) is also shown for comparison.

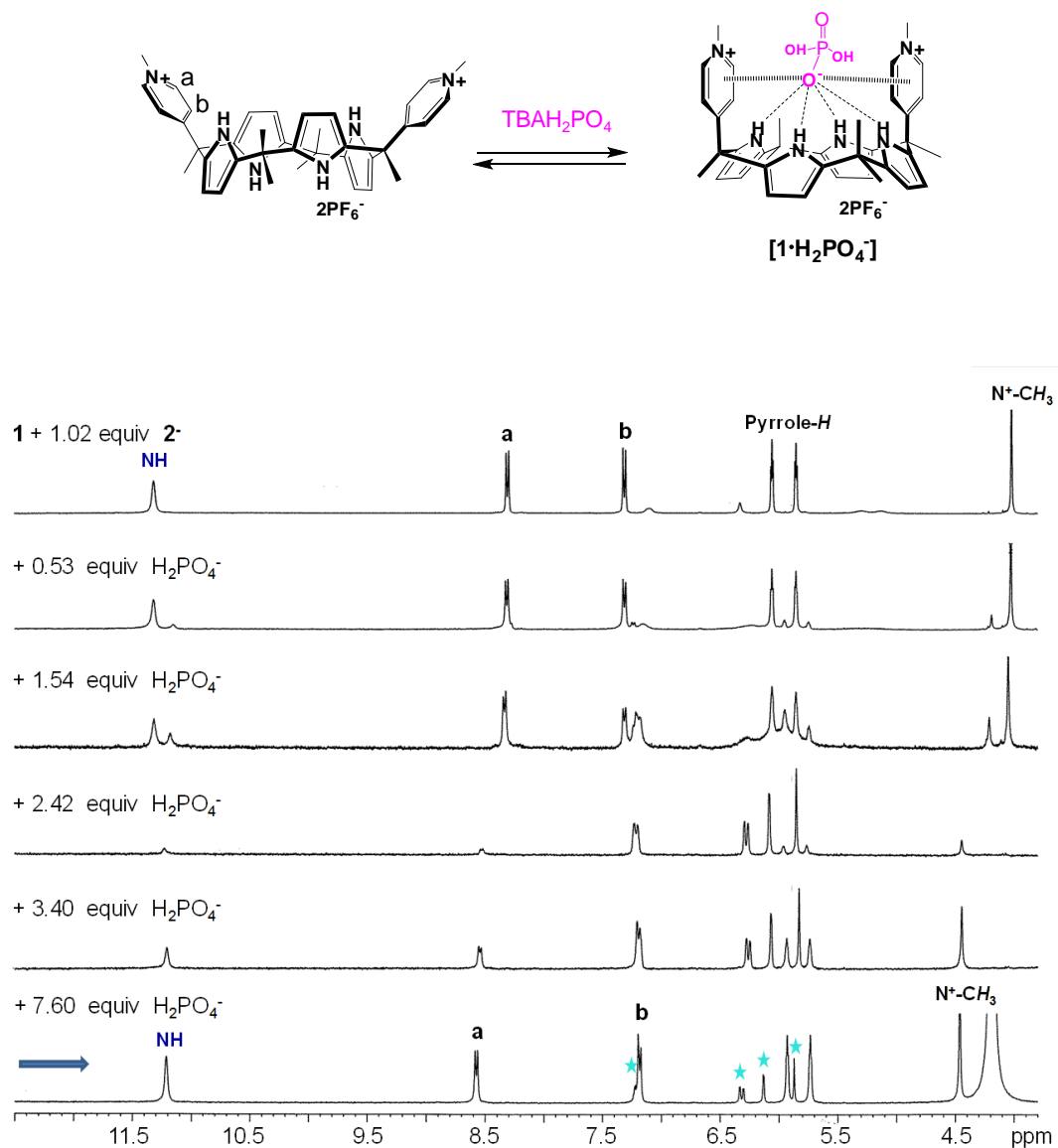
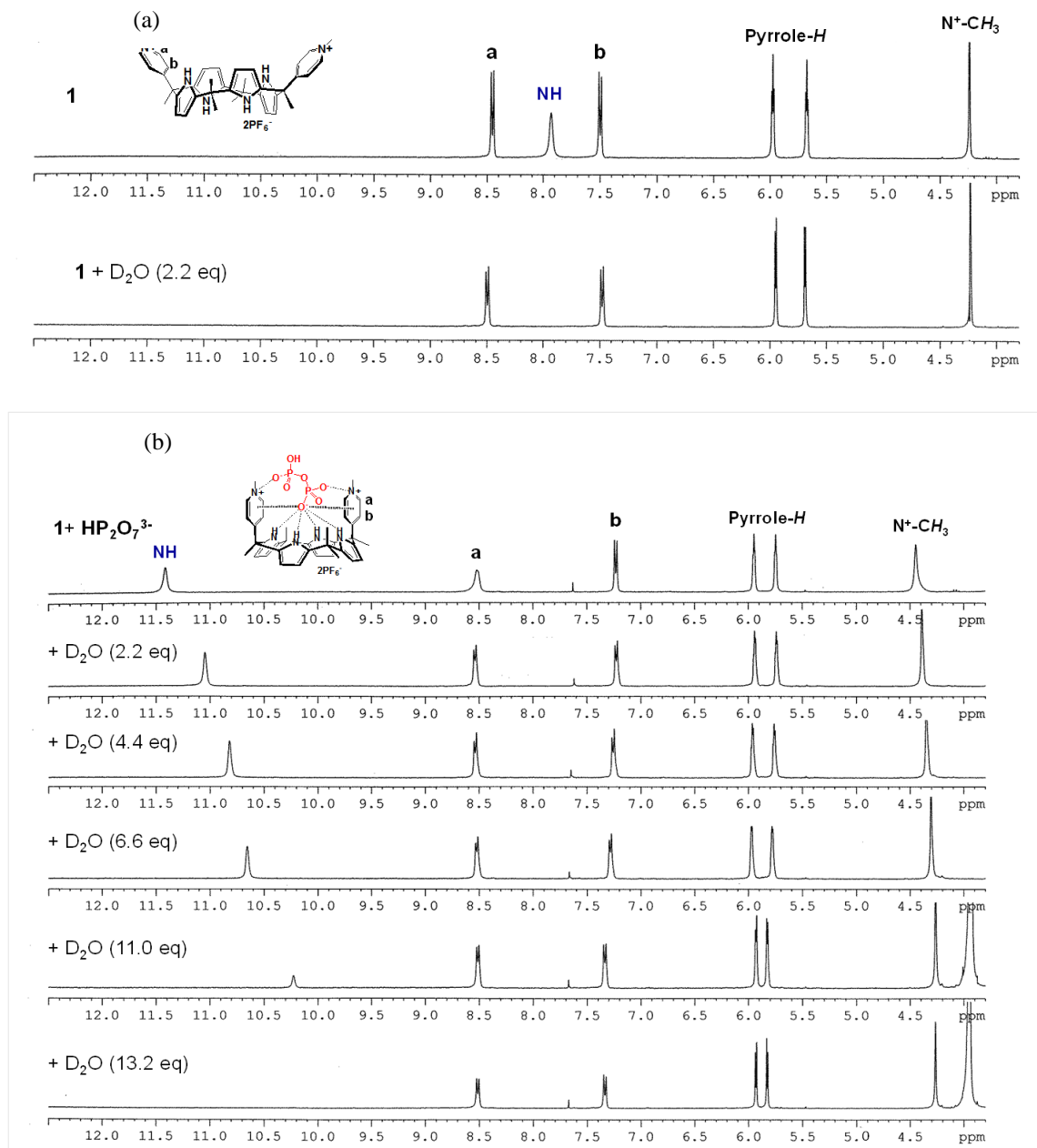
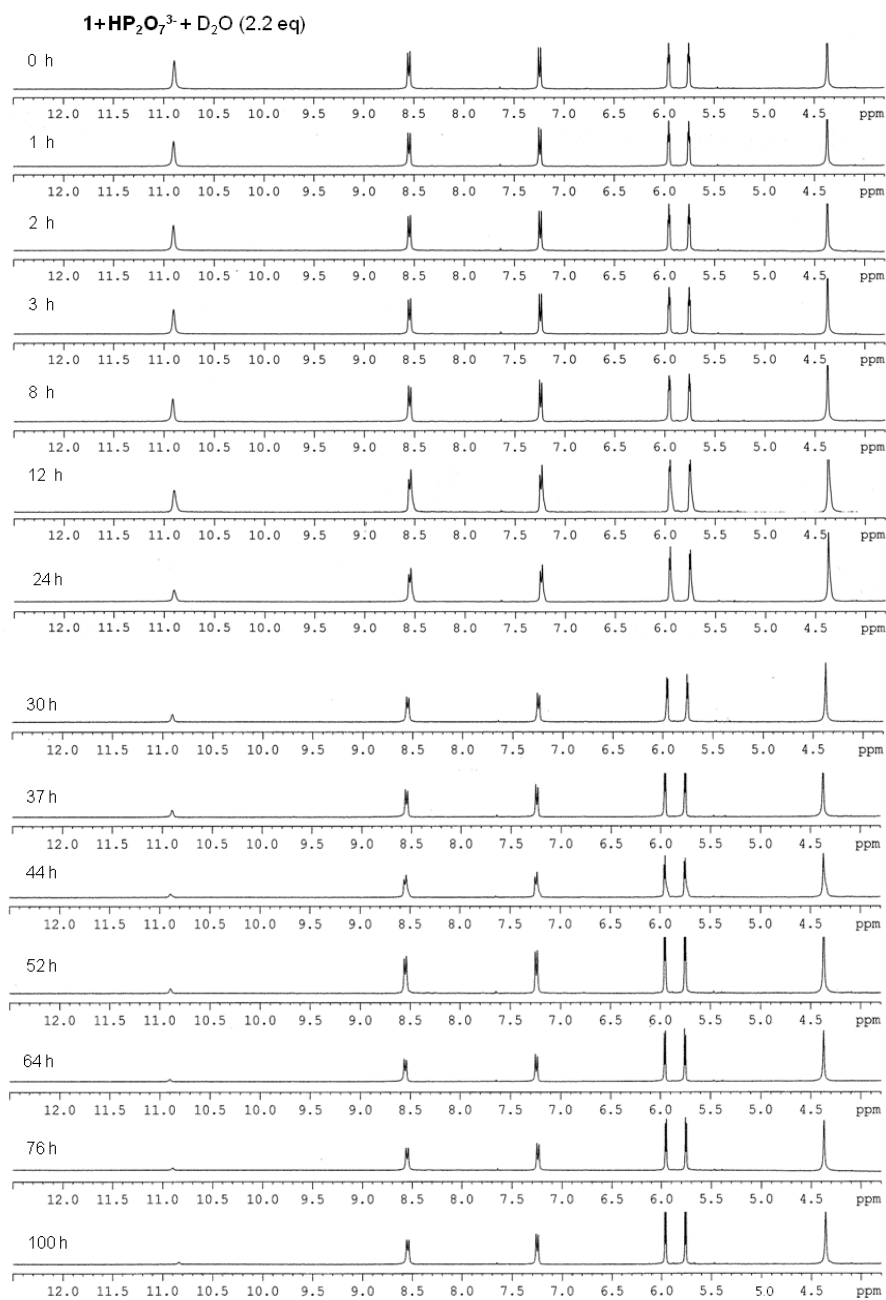


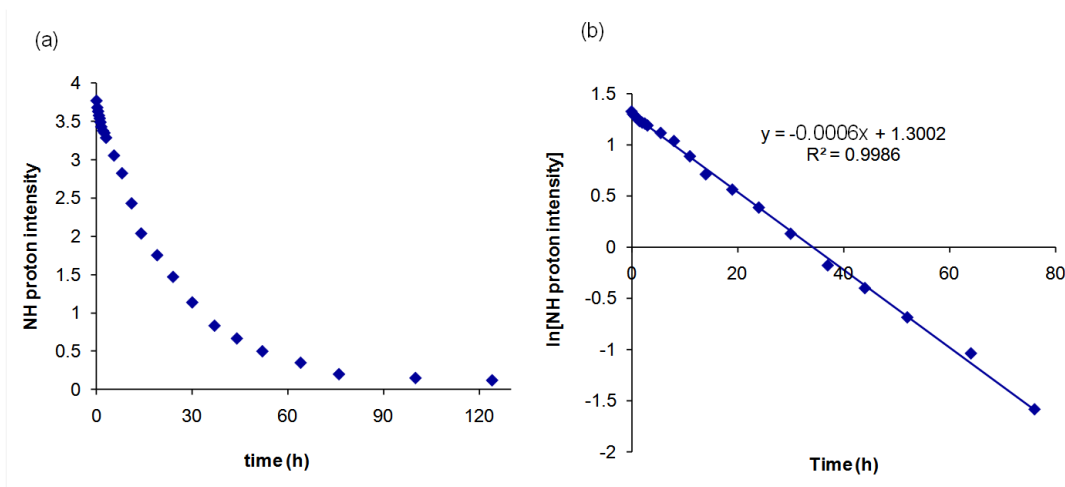
Figure S28. Partial ¹H NMR (300 MHz) spectra of the titration of receptor **1** (4.57 mM) with H₂PO₄⁻ (as its tetrabutylammonium salt) in CD₃CN.



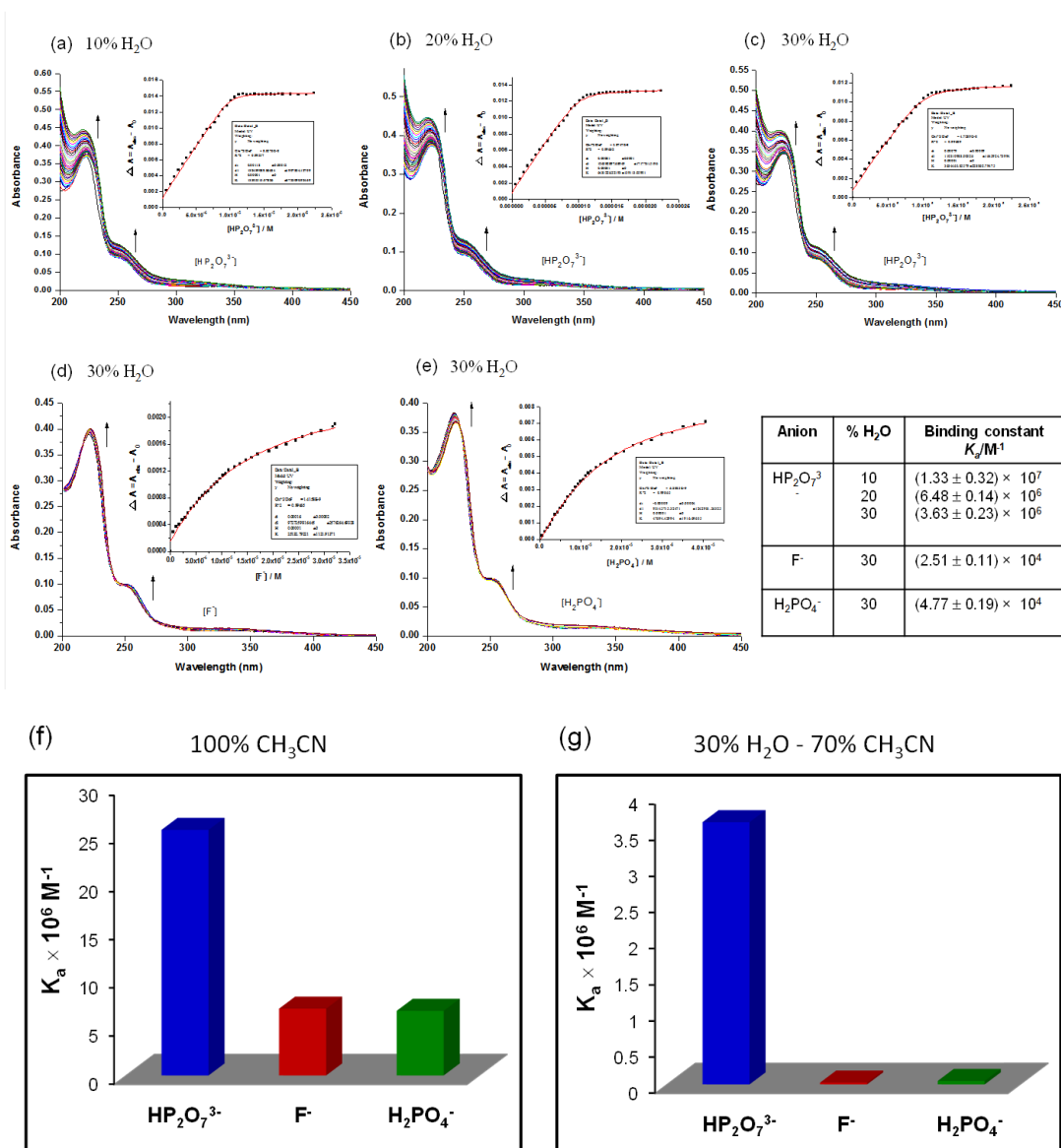
Supporting Figure S29: Partial ¹H NMR (300 MHz) spectra of CD₃CN solutions of (a) (top) **1** (4.57 mM) and (bottom) after adding 2.2 equiv. of D₂O. The complete disappearance of NH signal indicates that the H-D exchange is instantaneous; (b) (top) **1** (4.57 mM) + 1.45 equiv. of TBA₃HP₂O₇ and (second to last) after adding D₂O (2.2 equiv. – 13.2 equiv.). The requirement of excess D₂O for complete H-D exchange indicates that the NH protons are strongly involved in hydrogen bonding with pyrophosphate. All ¹H NMR spectra containing D₂O were recorded by shaking the tube vigorously for 10 seconds after the addition of D₂O.



Supporting Figure S30: Spectral monitoring of the changes in the ¹H NMR (300 MHz) spectra of CD₃CN solutions of **1** (4.57 mM) + 1.45 equiv. of TBA₃HP₂O₇ + 2.2 equiv. of D₂O with respect to various time intervals. The slow H-D exchange indicates that the NH protons are strongly involved in hydrogen bonding with pyrophosphate. Only selected spectra are shown here.

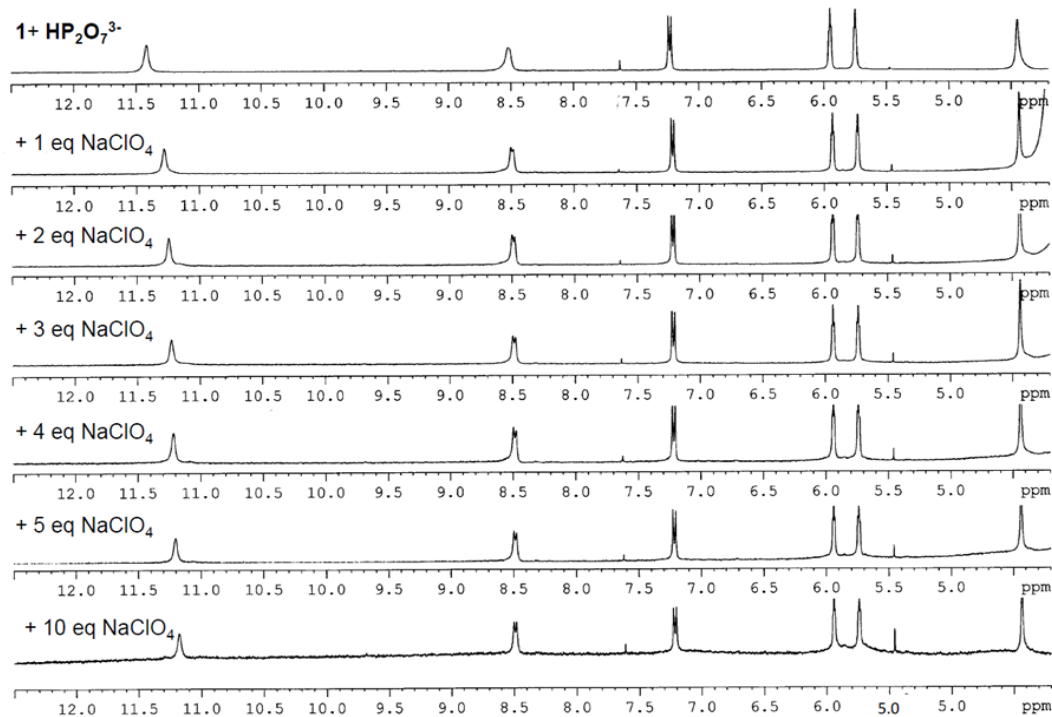


Supporting Figure S31: (a) Plot of NH proton intensity (obtained from the previous figure) *versus* time. (b) Its corresponding ln versus time plot. These plots provide support for the conclusion that the H-D exchange follows first order kinetics.

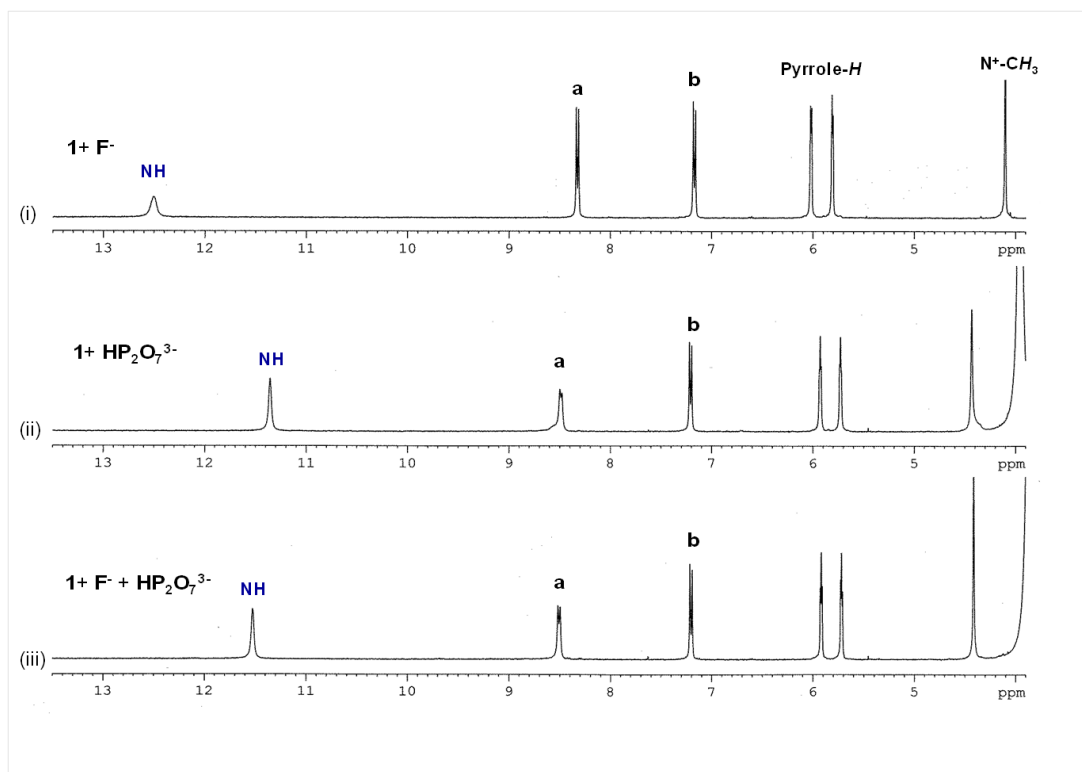


Supporting Figure S32: UV-vis absorption spectral changes of **1** (1.00×10^{-5} M) seen upon the addition of anion in: TBA₃HP₂O₇ (0 to 3 equiv.) (a) 10% water, (b) 20% water, (c) 30% water, (d) TBAF (0 to 4 equiv.) 30% water and (e) TBAH₂PO₄ (0 to 4 equiv.) 30% water-acetonitrile mixture at 25 °C. Inset shows their corresponding titration curves (plot of change in absorbance at 243 nm *versus* anion concentration). A comparison of their binding affinities K_a (f) in 100% acetonitrile and (g) 30% water-70% acetonitrile are also shown.

Competition Experiment



Supporting Figure S33: ¹H NMR spectra (300 MHz) of CD₃CN solutions of (top) **1** (4.57 mM) + 1.45 equiv. of TBA₃HP₂O₇ and (second to last) after adding NaClO₄ (0 – 10 equiv.). The persistence of hydrogen bonded NH signal even after addition of excess NaClO₄ indicates that the NH protons are in strong hydrogen bonding interactions with pyrophosphate and are not being decomplexed by the Na⁺ ion.



Supporting Figure S34: Competition experiment using ^1H NMR in CD_3CN . (i) **1** (4.57 mM) + 1.2 equiv. of TBAB, (ii) **1** (4.57 mM) + 1.2 equiv. of $\text{TBA}_3\text{HP}_2\text{O}_7$ and (iii) **1** (4.57 mM) + TBAB + $\text{TBA}_3\text{HP}_2\text{O}_7$ (1.2 equiv. of each). The persistence of the pyrophosphate hydrogen bonded NH signal in presence of equimolar amounts of fluoride is taken as evidence that the NH protons prefer hydrogen bonding interactions only with pyrophosphate, even in presence of the strong fluoride competitor. Thus the receptor can selectively recognize pyrophosphate anion in presence of fluoride.

Crystallographic Material for 1.

X-ray Experimental.

Table 1. Crystallographic Data for **1**.

Table 2. Fractional coordinates and equivalent isotropic thermal parameters (\AA^2) for the non-hydrogen atoms of **1**.

Table 3. Bond Lengths (\AA) and Angles ($^\circ$) for the non-hydrogen atoms of **1**.

Table 4. Anisotropic thermal parameters for the non-hydrogen atoms of **1**.

Table 5. Fractional coordinates and isotropic thermal parameters (\AA^2) for the hydrogen atoms of **1**.

Table 6. Torsion Angles ($^\circ$) for the non-hydrogen atoms of **1**.

Table 7. H-Bond Lengths (\AA) and Angles ($^\circ$) for **1**.

X-ray Experimental for $(C_{38}H_{44}N_6)^{2+} 2I^{-} - C_2H_3N - C_4H_{10}O$: Crystals grew as clusters of yellow laths by slow evaporation from acetonitrile and diethyl ether. The data crystal was cut from a larger crystal and had approximate dimensions; 0.17 x 0.07 x 0.05 mm. The data were collected on a Rigaku AFC12 diffractometer with a Saturn 724+ CCD using a graphite monochromator with MoK α radiation ($\lambda = 0.71073 \text{ \AA}$). A total of 2256 frames of data were collected using ω -scans with a scan range of 0.5° and a counting time of 18 seconds per frame. The data were collected at 100 K using a Rigaku XStream low temperature device. Details of crystal data, data collection and structure refinement are listed in Table 1. Data reduction were performed using the Rigaku Americas Corporation's Crystal Clear version 1.40.¹ The structure was solved by direct methods using SIR97² and refined by full-matrix least-squares on F² with anisotropic displacement parameters for the non-H atoms using SHELXL-97.³ The hydrogen atoms were calculated in ideal positions with isotropic displacement parameters set to 1.2xUeq of the attached atom (1.5xUeq for methyl hydrogen atoms).

A molecule of diethyl ether was disordered in such a way that the central oxygen atom appeared well behaved but the ethyl groups assumed two different conformations. The disorder was modeled by assigning the variable x to the site occupancy of one component of the disorder consisting of atoms, C1b, C2b, C4b, and C5b. The variable (1-x) was assigned to the comparable atoms of the alternate conformation, C1c, C2c, C4c and C5c. The geometry of these ethyl groups was restrained to be equivalent throughout the refinement. A common isotropic displacement parameter was refined while refining the variable x. In this way, the site occupancy of the major component of the disorder, C1b, C2b, C4b and C5b refined to 72(2)%.

In addition to the solvent disorder, one of the N-methyl pyridine groups also appeared to be disordered. The disorder manifested itself in highly elongated displacement parameters for the methyl carbon atom, C36, the pyridine nitrogen atom, N6, and atoms C33 and C34 of the ring. The disorder was modeled in a fashion similar to that for the ethyl ether molecule. Site occupancy factors for the major component refined to 53(2)% and consisted of atoms, N6a, C31a,

C32a, C33a, C34a, C35a and C36a.

The function, $\sum w(|F_o|^2 - |F_c|^2)^2$, was minimized, where $w = 1/[(\sigma(F_o))^2 + (0.0642 * P)^2 + (7.1395 * P)]$ and $P = (|F_o|^2 + 2|F_c|^2)/3$. $R_w(F^2)$ refined to 0.212, with $R(F)$ equal to 0.00977 and a goodness of fit, S , = 1.65. Definitions used for calculating $R(F)$, $R_w(F^2)$ and the goodness of fit, S , are given below.⁴ The data were checked for secondary extinction effects but no correction was necessary. Neutral atom scattering factors and values used to calculate the linear absorption coefficient are from the International Tables for X-ray Crystallography (1992).⁵ All figures were generated using SHELXTL/PC.⁶ Tables of positional and thermal parameters, bond lengths and angles, torsion angles and figures are found elsewhere.

Table 1. Crystal data and structure refinement for 1.

Empirical formula	C ₄₄ H ₅₇ I ₂ N ₇ O	
Formula weight	953.77	
Temperature	100(2) K	
Wavelength	0.71074 Å	
Crystal system	Monoclinic	
Space group	P21/c	
Unit cell dimensions	a = 9.2490(8) Å	α = 90°.
	b = 36.150(2) Å	β = 109.970(3)°.
	c = 14.6590(14) Å	γ = 90°.
Volume	4606.5(6) Å ³	
Z	4	
Density (calculated)	1.375 Mg/m ³	
Absorption coefficient	1.404 mm ⁻¹	
F(000)	1936	
Crystal size	0.17 x 0.07 x 0.05 mm	
Theta range for data collection	3.01 to 27.50°.	
Index ranges	-11 ≤ h ≤ 11, -46 ≤ k ≤ 46, -18 ≤ l ≤ 18	
Reflections collected	98870	
Independent reflections	10311 [R(int) = 0.0900]	
Completeness to theta = 27.50°	97.5 %	
Absorption correction	Semi-empirical from equivalents	
Max. and min. transmission	1.00 and 0.807	
Refinement method	Full-matrix least-squares on F ²	
Data / restraints / parameters	10311 / 446 / 582	
Goodness-of-fit on F ²	1.646	
Final R indices [I > 2σ(I)]	R1 = 0.0977, wR2 = 0.2019	
R indices (all data)	R1 = 0.1257, wR2 = 0.2116	
Largest diff. peak and hole	1.458 and -2.842 e.Å ⁻³	
CCDC deposit number	863400	

Table 2. Atomic coordinates ($\times 10^4$) and equivalent isotropic displacement parameters ($\text{\AA}^2 \times 10^3$). for 1. $U(\text{eq})$ is defined as one third of the trace of the orthogonalized U^{ij} tensor.

	x	y	z	$U(\text{eq})$
I1	284(1)	6387(1)	7036(1)	24(1)
I2	32(1)	6738(1)	1583(1)	65(1)
N1	2988(6)	6169(1)	9478(4)	19(1)
N2	2255(6)	5490(1)	7754(4)	17(1)
N3	3459(6)	6045(1)	6212(4)	18(1)
N4	4205(7)	6733(1)	7968(4)	21(1)
N5	-2610(6)	5790(2)	8788(4)	20(1)
C1	4058(8)	6415(2)	10034(5)	24(2)
C2	4901(9)	6216(2)	10821(5)	31(2)
C3	4311(8)	5853(2)	10775(5)	25(2)
C4	3126(7)	5827(2)	9935(5)	18(1)
C5	2089(7)	5508(2)	9498(4)	17(1)
C6	2544(7)	5333(2)	8670(5)	17(1)
C7	3318(8)	5006(2)	8650(5)	26(2)
C8	3480(9)	4970(2)	7706(5)	32(2)
C9	2812(7)	5268(2)	7161(5)	21(1)
C10	2653(8)	5364(2)	6099(5)	21(2)
C11	3729(8)	5669(2)	6050(5)	21(1)
C12	5114(8)	5662(2)	5885(5)	25(2)
C13	5688(8)	6030(2)	5936(5)	26(2)
C14	4655(7)	6263(2)	6145(5)	18(1)
C15	4729(8)	6673(2)	6331(5)	23(2)
C16	5198(8)	6754(2)	7406(5)	22(2)
C17	6599(9)	6836(2)	8027(6)	32(2)
C18	6456(9)	6869(2)	8983(5)	35(2)
C19	4983(9)	6811(2)	8934(5)	27(2)
C20	4188(9)	6811(2)	9713(5)	26(2)
C21	2232(8)	5208(2)	10291(5)	24(2)
C22	438(7)	5628(2)	9201(5)	17(1)
C23	-84(8)	5892(2)	9723(5)	21(1)

C24	-1591(8)	5970(2)	9507(5)	23(2)
C25	-2155(7)	5536(2)	8254(5)	20(1)
C26	-652(7)	5448(2)	8450(5)	22(2)
C27	-4249(8)	5872(2)	8578(5)	27(2)
C28	985(8)	5472(2)	5573(5)	29(2)
C29	3063(9)	5018(2)	5610(5)	30(2)
C30	5936(8)	6841(2)	5900(6)	28(2)
C31	3240(18)	6872(6)	5802(14)	23(2)
C32	2218(18)	6735(5)	4949(13)	29(3)
C33	845(17)	6909(4)	4536(11)	33(3)
N6	483(14)	7209(4)	4947(9)	34(2)
C34	1419(19)	7351(5)	5763(11)	33(2)
C35	2810(20)	7187(6)	6204(12)	26(2)
C36	-1011(19)	7390(6)	4484(14)	54(5)
C31A	3210(16)	6856(5)	5789(12)	22(2)
C32A	2454(16)	6734(4)	4856(12)	26(2)
C33A	1148(15)	6910(4)	4308(10)	30(2)
N6A	594(12)	7196(3)	4659(8)	33(2)
C34A	1263(17)	7324(4)	5543(10)	33(2)
C35A	2584(18)	7158(5)	6122(11)	28(2)
C36A	-819(18)	7385(5)	4067(12)	57(4)
C37	5167(11)	7031(2)	10599(6)	44(2)
C38	2611(9)	6989(2)	9371(5)	33(2)
O3B	6227(7)	8384(2)	8458(5)	60(2)
C1B	4691(16)	7834(3)	8193(12)	53(3)
C2B	4809(13)	8257(3)	8126(10)	56(3)
C4B	6506(15)	8745(3)	8530(11)	63(3)
C5B	8189(15)	8855(4)	8773(16)	71(4)
C1C	4210(30)	7930(8)	8080(40)	56(7)
C2C	5920(20)	8030(4)	8380(30)	50(5)
C4C	7608(19)	8526(6)	8760(30)	62(5)
C5C	7670(40)	8951(6)	8710(40)	66(7)
N1A	-2706(11)	4756(3)	7066(6)	68(3)
C1A	-2608(14)	4467(3)	6963(7)	64(3)
C2A	-2630(20)	4063(5)	6790(14)	150(7)

Table 3. Bond lengths [\AA] and angles [$^\circ$] for 1.

N1-C1	1.370(9)	C11-C12	1.383(10)
N1-C4	1.393(8)	C12-C13	1.426(10)
N1-H1	0.88	C12-H12	0.95
N2-C6	1.397(8)	C13-C14	1.384(9)
N2-C9	1.404(8)	C13-H13	0.95
N2-H2	0.88	C14-C15	1.504(9)
N3-C14	1.390(8)	C15-C31A	1.510(14)
N3-C11	1.416(8)	C15-C31	1.512(15)
N3-H3	0.88	C15-C16	1.513(10)
N4-C19	1.381(9)	C15-C30	1.580(9)
N4-C16	1.430(9)	C16-C17	1.338(10)
N4-H4	0.88	C17-C18	1.456(11)
N5-C24	1.321(9)	C17-H17	0.95
N5-C25	1.363(9)	C18-C19	1.356(11)
N5-C27	1.471(8)	C18-H18	0.95
C1-C2	1.357(10)	C19-C20	1.556(11)
C1-C20	1.524(9)	C20-C38	1.515(11)
C2-C3	1.413(10)	C20-C37	1.528(10)
C2-H2A	0.95	C21-H21A	0.98
C3-C4	1.343(10)	C21-H21B	0.98
C3-H3A	0.95	C21-H21C	0.98
C4-C5	1.495(9)	C22-C26	1.374(9)
C5-C22	1.501(9)	C22-C23	1.408(9)
C5-C6	1.550(9)	C23-C24	1.350(9)
C5-C21	1.563(9)	C23-H23	0.95
C6-C7	1.386(9)	C24-H24	0.95
C7-C8	1.447(10)	C25-C26	1.358(9)
C7-H7	0.95	C25-H25	0.95
C8-C9	1.358(9)	C26-H26	0.95
C8-H8	0.95	C27-H27A	0.98
C9-C10	1.551(9)	C27-H27B	0.98
C10-C11	1.503(10)	C27-H27C	0.98
C10-C28	1.521(9)	C28-H28A	0.98
C10-C29	1.553(9)	C28-H28B	0.98

C28-H28C	0.98	C37-H37B	0.98
C29-H29A	0.98	C37-H37C	0.98
C29-H29B	0.98	C38-H38A	0.98
C29-H29C	0.98	C38-H38B	0.98
C30-H30A	0.98	C38-H38C	0.98
C30-H30B	0.98	O3B-C4C	1.305(12)
C30-H30C	0.98	O3B-C2C	1.307(12)
C31-C32	1.376(12)	O3B-C2B	1.316(11)
C31-C35	1.400(11)	O3B-C4B	1.325(11)
C32-C33	1.360(13)	C1B-C2B	1.539(13)
C32-H32	0.95	C1B-H1B1	0.98
C33-N6	1.340(13)	C1B-H1B2	0.98
C33-H33	0.95	C1B-H1B3	0.98
N6-C34	1.318(13)	C2B-H2B1	0.99
N6-C36	1.468(14)	C2B-H2B2	0.99
C34-C35	1.365(12)	C4B-C5B	1.527(13)
C34-H34	0.95	C4B-H4B1	0.99
C35-H35	0.95	C4B-H4B2	0.99
C36-H36A	0.98	C5B-H5B1	0.98
C36-H36B	0.98	C5B-H5B2	0.98
C36-H36C	0.98	C5B-H5B3	0.98
C31A-C32A	1.378(12)	C1C-C2C	1.539(14)
C31A-C35A	1.400(11)	C1C-H1C1	0.98
C32A-C33A	1.358(13)	C1C-H1C2	0.98
C32A-H32A	0.95	C1C-H1C3	0.98
C33A-N6A	1.335(13)	C2C-H2C1	0.99
C33A-H33A	0.95	C2C-H2C2	0.99
N6A-C34A	1.314(13)	C4C-C5C	1.540(14)
N6A-C36A	1.466(13)	C4C-H4C1	0.99
C34A-C35A	1.366(12)	C4C-H4C2	0.99
C34A-H34A	0.95	C5C-H5C1	0.98
C35A-H35A	0.95	C5C-H5C2	0.98
C36A-H36D	0.98	C5C-H5C3	0.98
C36A-H36E	0.98	N1A-C1A	1.065(13)
C36A-H36F	0.98	C1A-C2A	1.481(19)
C37-H37A	0.98	C2A-H2A1	0.98

C2A-H2A2	0.98	C2A-H2A3	0.98
C1-N1-C4	111.1(5)	C7-C6-C5	130.3(6)
C1-N1-H1	124.4	N2-C6-C5	124.9(5)
C4-N1-H1	124.4	C6-C7-C8	108.7(6)
C6-N2-C9	111.9(5)	C6-C7-H7	125.7
C6-N2-H2	124.0	C8-C7-H7	125.7
C9-N2-H2	124.0	C9-C8-C7	108.4(6)
C14-N3-C11	110.1(5)	C9-C8-H8	125.8
C14-N3-H3	125.0	C7-C8-H8	125.8
C11-N3-H3	125.0	C8-C9-N2	106.1(6)
C19-N4-C16	111.6(6)	C8-C9-C10	129.5(6)
C19-N4-H4	124.2	N2-C9-C10	124.4(6)
C16-N4-H4	124.2	C11-C10-C28	111.2(6)
C24-N5-C25	121.0(6)	C11-C10-C9	112.0(5)
C24-N5-C27	118.0(6)	C28-C10-C9	107.4(6)
C25-N5-C27	121.0(6)	C11-C10-C29	107.4(6)
C2-C1-N1	104.6(6)	C28-C10-C29	109.7(6)
C2-C1-C20	132.6(7)	C9-C10-C29	109.2(5)
N1-C1-C20	122.7(6)	C12-C11-N3	105.9(6)
C1-C2-C3	110.5(7)	C12-C11-C10	131.5(6)
C1-C2-H2A	124.7	N3-C11-C10	122.5(6)
C3-C2-H2A	124.7	C11-C12-C13	108.9(6)
C4-C3-C2	106.9(6)	C11-C12-H12	125.6
C4-C3-H3A	126.6	C13-C12-H12	125.6
C2-C3-H3A	126.6	C14-C13-C12	107.9(6)
C3-C4-N1	106.9(6)	C14-C13-H13	126.1
C3-C4-C5	130.6(6)	C12-C13-H13	126.1
N1-C4-C5	122.6(6)	C13-C14-N3	107.3(6)
C4-C5-C22	110.1(5)	C13-C14-C15	130.3(6)
C4-C5-C6	110.2(5)	N3-C14-C15	122.3(6)
C22-C5-C6	114.3(5)	C14-C15-C31A	111.1(9)
C4-C5-C21	109.7(5)	C14-C15-C31	113.5(10)
C22-C5-C21	103.5(5)	C14-C15-C16	111.0(5)
C6-C5-C21	108.7(5)	C31A-C15-C16	110.3(9)
C7-C6-N2	104.9(6)	C31-C15-C16	109.2(9)

C14-C15-C30	107.5(6)	C23-C24-H24	120.6
C31A-C15-C30	106.1(9)	C26-C25-N5	122.0(6)
C31-C15-C30	104.8(9)	C26-C25-H25	119.0
C16-C15-C30	110.6(6)	N5-C25-H25	119.0
C17-C16-N4	106.4(6)	C25-C26-C22	118.5(7)
C17-C16-C15	128.2(7)	C25-C26-H26	120.7
N4-C16-C15	125.3(6)	C22-C26-H26	120.7
C16-C17-C18	106.7(7)	N5-C27-H27A	109.5
C16-C17-H17	126.6	N5-C27-H27B	109.5
C18-C17-H17	126.6	H27A-C27-H27B	109.5
C19-C18-C17	110.9(7)	N5-C27-H27C	109.5
C19-C18-H18	124.6	H27A-C27-H27C	109.5
C17-C18-H18	124.6	H27B-C27-H27C	109.5
C18-C19-N4	104.4(6)	C10-C28-H28A	109.5
C18-C19-C20	132.8(7)	C10-C28-H28B	109.5
N4-C19-C20	122.8(6)	H28A-C28-H28B	109.5
C38-C20-C1	109.4(6)	C10-C28-H28C	109.5
C38-C20-C37	106.5(6)	H28A-C28-H28C	109.5
C1-C20-C37	108.2(6)	H28B-C28-H28C	109.5
C38-C20-C19	113.5(6)	C10-C29-H29A	109.5
C1-C20-C19	109.5(6)	C10-C29-H29B	109.5
C37-C20-C19	109.4(6)	H29A-C29-H29B	109.5
C5-C21-H21A	109.5	C10-C29-H29C	109.5
C5-C21-H21B	109.5	H29A-C29-H29C	109.5
H21A-C21-H21B	109.5	H29B-C29-H29C	109.5
C5-C21-H21C	109.5	C15-C30-H30A	109.5
H21A-C21-H21C	109.5	C15-C30-H30B	109.5
H21B-C21-H21C	109.5	H30A-C30-H30B	109.5
C26-C22-C23	117.5(6)	C15-C30-H30C	109.5
C26-C22-C5	119.5(6)	H30A-C30-H30C	109.5
C23-C22-C5	122.7(6)	H30B-C30-H30C	109.5
C24-C23-C22	122.2(6)	C32-C31-C35	118.0(10)
C24-C23-H23	118.9	C32-C31-C15	121.2(13)
C22-C23-H23	118.9	C35-C31-C15	120.6(13)
N5-C24-C23	118.8(6)	C33-C32-C31	119.1(11)
N5-C24-H24	120.6	C33-C32-H32	120.5

C31-C32-H32	120.5	H36E-C36A-H36F	109.5
N6-C33-C32	120.9(11)	C20-C37-H37A	109.5
N6-C33-H33	119.6	C20-C37-H37B	109.5
C32-C33-H33	119.6	H37A-C37-H37B	109.5
C34-N6-C33	122.5(10)	C20-C37-H37C	109.5
C34-N6-C36	118.0(12)	H37A-C37-H37C	109.5
C33-N6-C36	119.5(12)	H37B-C37-H37C	109.5
N6-C34-C35	118.8(10)	C20-C38-H38A	109.5
N6-C34-H34	120.6	C20-C38-H38B	109.5
C35-C34-H34	120.6	H38A-C38-H38B	109.5
C34-C35-C31	120.8(10)	C20-C38-H38C	109.5
C34-C35-H35	119.6	H38A-C38-H38C	109.5
C31-C35-H35	119.6	H38B-C38-H38C	109.5
C32A-C31A-C35A	117.7(9)	C4C-O3B-C2C	124.7(13)
C32A-C31A-C15	116.6(12)	C4C-O3B-C2B	176.9(13)
C35A-C31A-C15	125.4(12)	C2C-O3B-C2B	57.9(12)
C33A-C32A-C31A	119.0(10)	C4C-O3B-C4B	56.4(12)
C33A-C32A-H32A	120.5	C2C-O3B-C4B	178.9(10)
C31A-C32A-H32A	120.5	C2B-O3B-C4B	120.9(9)
N6A-C33A-C32A	121.0(10)	O3B-C2B-C1B	114.0(9)
N6A-C33A-H33A	119.5	O3B-C2B-H2B1	108.8
C32A-C33A-H33A	119.5	C1B-C2B-H2B1	108.8
C34A-N6A-C33A	122.6(9)	O3B-C2B-H2B2	108.8
C34A-N6A-C36A	116.4(11)	C1B-C2B-H2B2	108.8
C33A-N6A-C36A	120.9(11)	H2B1-C2B-H2B2	107.7
N6A-C34A-C35A	118.6(10)	O3B-C4B-C5B	115.5(9)
N6A-C34A-H34A	120.7	O3B-C4B-H4B1	108.4
C35A-C34A-H34A	120.7	C5B-C4B-H4B1	108.4
C34A-C35A-C31A	121.0(10)	O3B-C4B-H4B2	108.4
C34A-C35A-H35A	119.5	C5B-C4B-H4B2	108.4
C31A-C35A-H35A	119.5	H4B1-C4B-H4B2	107.5
N6A-C36A-H36D	109.5	C2C-C1C-H1C1	109.5
N6A-C36A-H36E	109.5	C2C-C1C-H1C2	109.5
H36D-C36A-H36E	109.5	H1C1-C1C-H1C2	109.5
N6A-C36A-H36F	109.5	C2C-C1C-H1C3	109.5
H36D-C36A-H36F	109.5	H1C1-C1C-H1C3	109.5

H1C2-C1C-H1C3	109.5	C4C-C5C-H5C1	109.4
O3B-C2C-C1C	115.2(11)	C4C-C5C-H5C2	109.5
O3B-C2C-H2C1	108.5	H5C1-C5C-H5C2	109.5
C1C-C2C-H2C1	108.5	C4C-C5C-H5C3	109.5
O3B-C2C-H2C2	108.5	H5C1-C5C-H5C3	109.5
C1C-C2C-H2C2	108.5	H5C2-C5C-H5C3	109.5
H2C1-C2C-H2C2	107.5	N1A-C1A-C2A	174.5(16)
O3B-C4C-C5C	114.9(12)	C1A-C2A-H2A1	109.5
O3B-C4C-H4C1	108.5	C1A-C2A-H2A2	109.5
C5C-C4C-H4C1	108.6	H2A1-C2A-H2A2	109.5
O3B-C4C-H4C2	108.6	C1A-C2A-H2A3	109.5
C5C-C4C-H4C2	108.5	H2A1-C2A-H2A3	109.5
H4C1-C4C-H4C2	107.5	H2A2-C2A-H2A3	109.5

Table 4. Anisotropic displacement parameters ($\text{\AA}^2 \times 10^3$) for 1. The anisotropic displacement factor exponent takes the form: $-2\pi^2 [h^2 a^{*2} U^{11} + \dots + 2 h k a^* b^* U^{12}]$

	U^{11}	U^{22}	U^{33}	U^{23}	U^{13}	U^{12}
I1	15(1)	23(1)	31(1)	5(1)	7(1)	6(1)
I2	76(1)	61(1)	50(1)	-4(1)	12(1)	-12(1)
N1	20(3)	21(3)	17(3)	1(2)	6(2)	3(2)
N2	11(3)	17(3)	19(3)	2(2)	1(2)	2(2)
N3	15(3)	20(3)	17(3)	1(2)	6(2)	7(2)
N4	18(3)	19(3)	25(3)	-4(2)	7(3)	-3(2)
N5	16(3)	23(3)	21(3)	8(2)	8(2)	1(2)
C1	33(4)	22(3)	17(3)	-5(3)	9(3)	-7(3)
C2	34(5)	28(4)	24(4)	-8(3)	2(4)	-4(3)
C3	27(4)	24(4)	19(4)	5(3)	4(3)	6(3)
C4	20(3)	17(3)	19(3)	2(3)	10(3)	1(3)
C5	15(3)	18(3)	16(3)	4(2)	4(3)	1(2)
C6	18(3)	13(3)	18(3)	5(2)	3(3)	0(2)
C7	33(4)	21(3)	21(4)	4(3)	5(3)	11(3)
C8	44(5)	21(4)	32(4)	1(3)	15(4)	18(3)
C9	18(3)	20(3)	22(4)	-2(3)	4(3)	1(3)
C10	23(4)	20(3)	16(3)	-4(3)	1(3)	5(3)
C11	26(4)	24(3)	11(3)	1(3)	4(3)	9(3)
C12	29(4)	25(4)	22(4)	2(3)	9(3)	14(3)
C13	20(4)	32(4)	28(4)	1(3)	12(3)	8(3)
C14	17(3)	20(3)	16(3)	3(3)	5(3)	6(3)
C15	23(4)	18(3)	27(4)	3(3)	9(3)	1(3)
C16	25(4)	16(3)	23(4)	5(3)	6(3)	0(3)
C17	23(4)	33(4)	37(5)	0(3)	8(4)	-9(3)
C18	34(5)	40(5)	22(4)	-1(3)	-1(4)	-17(4)
C19	37(4)	19(3)	18(4)	-4(3)	1(3)	-8(3)
C20	37(4)	21(4)	19(4)	-5(3)	7(3)	-7(3)
C21	26(4)	23(3)	26(4)	7(3)	13(3)	3(3)
C22	17(3)	16(3)	17(3)	8(2)	5(3)	0(2)
C23	18(4)	22(3)	23(4)	1(3)	6(3)	1(3)
C24	19(4)	27(4)	22(4)	1(3)	6(3)	3(3)

C25	14(3)	20(3)	24(4)	5(3)	5(3)	-3(3)
C26	19(4)	20(3)	26(4)	9(3)	8(3)	-1(3)
C27	15(4)	34(4)	29(4)	4(3)	2(3)	4(3)
C28	30(4)	25(4)	22(4)	0(3)	-3(3)	-1(3)
C29	42(5)	22(4)	20(4)	-5(3)	4(3)	5(3)
C30	21(4)	29(4)	36(4)	9(3)	13(3)	1(3)
C31	24(3)	24(3)	24(3)	3(3)	10(3)	3(3)
C32	28(4)	30(3)	28(4)	3(3)	9(3)	5(3)
C33	32(4)	37(4)	30(4)	4(3)	10(3)	6(3)
N6	32(3)	35(3)	33(4)	5(3)	10(3)	10(3)
C34	34(4)	31(4)	33(4)	2(3)	11(3)	8(3)
C35	26(4)	25(4)	28(4)	3(3)	11(3)	3(3)
C36	49(7)	57(7)	52(8)	10(7)	12(6)	16(6)
C31A	24(3)	23(3)	23(3)	4(3)	10(3)	3(3)
C32A	26(4)	29(3)	26(3)	3(3)	10(3)	6(3)
C33A	30(4)	35(3)	27(4)	4(3)	12(3)	8(3)
N6A	34(3)	35(3)	30(4)	2(3)	9(3)	11(3)
C34A	35(4)	30(3)	33(4)	1(3)	11(3)	8(3)
C35A	29(4)	27(3)	28(3)	2(3)	11(3)	3(3)
C36A	56(7)	64(7)	45(7)	-1(6)	10(6)	28(6)
C37	72(7)	29(4)	31(4)	-11(3)	17(5)	-20(4)
C38	54(5)	21(4)	29(4)	-2(3)	21(4)	3(3)
O3B	75(5)	46(4)	47(4)	-2(3)	6(3)	-12(3)
C1B	73(8)	45(6)	36(6)	-4(5)	13(6)	-6(6)
C2B	59(6)	55(5)	54(5)	0(5)	20(5)	-3(5)
C4B	68(6)	63(6)	58(6)	-4(5)	23(5)	-3(5)
C5B	67(8)	53(7)	79(8)	-11(7)	10(7)	0(6)
N1A	89(7)	66(6)	38(5)	-11(4)	7(5)	11(5)
C1A	88(7)	54(6)	45(5)	-5(4)	14(5)	23(5)
C2A	195(15)	93(11)	144(13)	-25(10)	35(11)	32(11)

Table 5. Hydrogen coordinates ($\times 10^4$) and isotropic displacement parameters ($\text{\AA}^2 \times 10^{-3}$) for 1.

	x	y	z	U(eq)
H1	2304	6222	8907	23
H2	1781	5702	7571	20
H3	2651	6128	6336	21
H4	3221	6677	7728	25
H2A	5767	6307	11332	37
H3A	4682	5664	11247	29
H7	3682	4835	9169	31
H8	3970	4772	7503	38
H12	5603	5446	5758	30
H13	6615	6103	5843	31
H17	7511	6867	7875	38
H18	7283	6923	9562	42
H21A	1955	5317	10822	36
H21B	3294	5117	10544	36
H21C	1537	5002	10005	36
H23	649	6019	10245	26
H24	-1913	6152	9864	27
H25	-2914	5416	7729	24
H26	-360	5267	8076	26
H27A	-4541	5805	9140	41
H27B	-4869	5730	8010	41
H27C	-4430	6137	8446	41
H28A	762	5705	5842	44
H28B	306	5277	5659	44
H28C	813	5504	4880	44
H29A	2913	5073	4929	45
H29B	2395	4811	5643	45
H29C	4139	4950	5949	45
H30A	5942	7111	5956	42
H30B	5652	6772	5214	42

H30C	6962	6744	6260	42
H32	2468	6522	4653	35
H33	133	6816	3947	40
H34	1130	7564	6039	39
H35	3501	7287	6790	31
H36A	-1477	7446	4976	81
H36B	-1690	7224	3995	81
H36C	-864	7619	4172	81
H32A	2842	6531	4599	32
H33A	620	6827	3664	36
H34A	836	7527	5775	39
H35A	3087	7249	6760	33
H36D	-849	7633	4327	85
H36E	-1714	7243	4083	85
H36F	-839	7403	3396	85
H37A	5254	7287	10409	66
H37B	6194	6920	10860	66
H37C	4680	7025	11097	66
H38A	1950	6861	8787	49
H38B	2706	7250	9221	49
H38C	2156	6970	9883	49
H1B1	5175	7716	7768	79
H1B2	3606	7762	7990	79
H1B3	5217	7755	8865	79
H2B1	4333	8333	7439	67
H2B2	4212	8374	8496	67
H4B1	6135	8846	9038	75
H4B2	5897	8862	7908	75
H5B1	8829	8712	9333	106
H5B2	8307	9120	8926	106
H5B3	8511	8804	8214	106
H1C1	3729	8074	8465	83
H1C2	4102	7665	8191	83
H1C3	3697	7985	7389	83
H2C1	6475	7911	9012	60
H2C2	6338	7924	7896	60

H4C1	8187	8422	8359	74
H4C2	8140	8447	9437	74
H5C1	7181	9033	8040	99
H5C2	8739	9033	8957	99
H5C3	7112	9057	9114	99
H2A1	-3313	3944	7089	224
H2A2	-1590	3963	7077	224
H2A3	-3014	4015	6090	224

Table 6. Torsion angles [°] for 1.

C4-N1-C1-C2	2.5(8)	C8-C9-C10-C29	12.8(10)
C4-N1-C1-C20	179.5(6)	N2-C9-C10-C29	-167.2(6)
N1-C1-C2-C3	-2.7(8)	C14-N3-C11-C12	0.1(7)
C20-C1-C2-C3	-179.2(7)	C14-N3-C11-C10	178.5(6)
C1-C2-C3-C4	2.0(9)	C28-C10-C11-C12	-137.7(7)
C2-C3-C4-N1	-0.4(8)	C9-C10-C11-C12	102.3(8)
C2-C3-C4-C5	179.1(7)	C29-C10-C11-C12	-17.6(10)
C1-N1-C4-C3	-1.4(8)	C28-C10-C11-N3	44.4(8)
C1-N1-C4-C5	179.1(6)	C9-C10-C11-N3	-75.7(7)
C3-C4-C5-C22	129.5(7)	C29-C10-C11-N3	164.4(6)
N1-C4-C5-C22	-51.1(8)	N3-C11-C12-C13	-0.5(7)
C3-C4-C5-C6	-103.5(8)	C10-C11-C12-C13	-178.7(6)
N1-C4-C5-C6	75.9(7)	C11-C12-C13-C14	0.7(8)
C3-C4-C5-C21	16.1(10)	C12-C13-C14-N3	-0.6(8)
N1-C4-C5-C21	-164.5(6)	C12-C13-C14-C15	176.4(7)
C9-N2-C6-C7	0.7(7)	C11-N3-C14-C13	0.4(7)
C9-N2-C6-C5	179.5(6)	C11-N3-C14-C15	-177.0(6)
C4-C5-C6-C7	104.6(8)	C13-C14-C15-C31A	135.3(10)
C22-C5-C6-C7	-130.7(7)	N3-C14-C15-C31A	-48.1(11)
C21-C5-C6-C7	-15.6(9)	C13-C14-C15-C31	135.0(11)
C4-C5-C6-N2	-73.8(7)	N3-C14-C15-C31	-48.4(12)
C22-C5-C6-N2	50.8(8)	C13-C14-C15-C16	-101.5(8)
C21-C5-C6-N2	165.9(6)	N3-C14-C15-C16	75.1(8)
N2-C6-C7-C8	-0.3(8)	C13-C14-C15-C30	19.6(10)
C5-C6-C7-C8	-179.0(7)	N3-C14-C15-C30	-163.8(6)
C6-C7-C8-C9	-0.2(9)	C19-N4-C16-C17	1.4(8)
C7-C8-C9-N2	0.6(8)	C19-N4-C16-C15	177.9(6)
C7-C8-C9-C10	-179.4(7)	C14-C15-C16-C17	97.3(8)
C6-N2-C9-C8	-0.8(8)	C31A-C15-C16-C17	-139.1(10)
C6-N2-C9-C10	179.2(6)	C31-C15-C16-C17	-136.8(11)
C8-C9-C10-C11	-106.0(8)	C30-C15-C16-C17	-21.9(9)
N2-C9-C10-C11	74.0(8)	C14-C15-C16-N4	-78.4(8)
C8-C9-C10-C28	131.8(8)	C31A-C15-C16-N4	45.2(11)
N2-C9-C10-C28	-48.2(8)	C31-C15-C16-N4	47.5(11)

C30-C15-C16-N4	162.3(6)	C14-C15-C31-C32	-26.9(15)
N4-C16-C17-C18	-0.5(8)	C31A-C15-C31-C32	-33(33)
C15-C16-C17-C18	-176.8(6)	C16-C15-C31-C32	-151.4(10)
C16-C17-C18-C19	-0.6(9)	C30-C15-C31-C32	90.1(12)
C17-C18-C19-N4	1.5(8)	C14-C15-C31-C35	148.5(9)
C17-C18-C19-C20	179.8(7)	C31A-C15-C31-C35	142(34)
C16-N4-C19-C18	-1.8(8)	C16-C15-C31-C35	24.0(12)
C16-N4-C19-C20	179.7(6)	C30-C15-C31-C35	-94.5(10)
C2-C1-C20-C38	-135.0(9)	C35-C31-C32-C33	-0.2(3)
N1-C1-C20-C38	49.0(9)	C15-C31-C32-C33	175.3(15)
C2-C1-C20-C37	-19.3(12)	C31-C32-C33-N6	0.1(3)
N1-C1-C20-C37	164.7(7)	C32-C33-N6-C34	-0.1(7)
C2-C1-C20-C19	100.0(9)	C32-C33-N6-C36	-179.8(4)
N1-C1-C20-C19	-76.1(8)	C33-N6-C34-C35	0.2(9)
C18-C19-C20-C38	140.2(8)	C36-N6-C34-C35	179.9(5)
N4-C19-C20-C38	-41.7(9)	N6-C34-C35-C31	-0.4(9)
C18-C19-C20-C1	-97.1(9)	C32-C31-C35-C34	0.4(6)
N4-C19-C20-C1	81.0(8)	C15-C31-C35-C34	-175.2(15)
C18-C19-C20-C37	21.4(11)	C14-C15-C31A-C32A	-40.8(12)
N4-C19-C20-C37	-160.5(7)	C31-C15-C31A-C32A	133(34)
C4-C5-C22-C26	152.4(6)	C16-C15-C31A-C32A	-164.4(8)
C6-C5-C22-C26	27.7(8)	C30-C15-C31A-C32A	75.8(11)
C21-C5-C22-C26	-90.4(7)	C14-C15-C31A-C35A	145.2(8)
C4-C5-C22-C23	-34.4(8)	C31-C15-C31A-C35A	-41(34)
C6-C5-C22-C23	-159.1(6)	C16-C15-C31A-C35A	21.7(12)
C21-C5-C22-C23	82.8(7)	C30-C15-C31A-C35A	-98.2(10)
C26-C22-C23-C24	-0.1(9)	C35A-C31A-C32A-C33A	-0.3(3)
C5-C22-C23-C24	-173.4(6)	C15-C31A-C32A-C33A	-174.7(13)
C25-N5-C24-C23	-1.8(10)	C31A-C32A-C33A-N6A	0.1(3)
C27-N5-C24-C23	178.5(6)	C32A-C33A-N6A-C34A	-0.2(7)
C22-C23-C24-N5	0.9(10)	C32A-C33A-N6A-C36A	-179.8(4)
C24-N5-C25-C26	2.0(9)	C33A-N6A-C34A-C35A	0.5(9)
C27-N5-C25-C26	-178.3(6)	C36A-N6A-C34A-C35A	-179.9(5)
N5-C25-C26-C22	-1.1(9)	N6A-C34A-C35A-C31A	-0.7(8)
C23-C22-C26-C25	0.2(9)	C32A-C31A-C35A-C34A	0.6(6)
C5-C22-C26-C25	173.7(6)	C15-C31A-C35A-C34A	174.4(14)

C2C-O3B-C2B-C1B	6(2)	C4C-O3B-C2C-C1C	176(3)
C4B-O3B-C2B-C1B	-173.8(12)	C2B-O3B-C2C-C1C	-6(3)
C4C-O3B-C4B-C5B	7(2)	C2C-O3B-C4C-C5C	176(3)
C2B-O3B-C4B-C5B	-170.8(14)	C4B-O3B-C4C-C5C	-4(3)

Table 7. Hydrogen bonds for 1 [Å and °].

D-H...A	d(D-H)	d(H...A)	d(D...A)	<(DHA)
N1-H1...I1	0.88	2.81	3.684(5)	176
N2-H2...I1	0.88	2.81	3.694(5)	179
N3-H3...I1	0.88	2.87	3.747(5)	172
N4-H4...I1	0.88	2.76	3.633(6)	171

Symmetry transformations used to generate equivalent atoms:

References

- 1) CrystalClear 1.40 (2008). Rigaku Americas Corporation, The Woodlands, TX.
- 2) SIR97. (1999). A program for crystal structure solution. Altomare A., Burla M.C., Camalli M., Cascarano G.L., Giacovazzo C., Guagliardi A., Moliterni A.G.G., Polidori G., Spagna R. J. Appl. Cryst. 32, 115-119.
- 3) Sheldrick, G. M. (1994). SHELXL97. Program for the Refinement of Crystal Structures. University of Gottingen, Germany.
- 4) $R_w(F^2) = \{\sum w(|F_o|^2 - |F_c|^2)^2 / \sum w(|F_o|^4)\}^{1/2}$ where w is the weight given each reflection.
 $R(F) = \sum(|F_o| - |F_c|) / \sum |F_o|$ for reflections with $F_o > 4(\sigma(F_o))$.
 $S = [\sum w(|F_o|^2 - |F_c|^2)^2 / (n - p)]^{1/2}$, where n is the number of reflections and p is the number of refined parameters.
- 5) International Tables for X-ray Crystallography (1992). Vol. C, Tables 4.2.6.8 and 6.1.1.4, A. J. C. Wilson, editor, Boston: Kluwer Academic Press.
- 6) Sheldrick, G. M. (1994). SHELXTL/PC (Version 5.03). Siemens Analytical X-ray Instruments, Inc., Madison, Wisconsin, USA.